Induction of IAPP amyloid deposition and associated diabetic abnormalities by a prion-like mechanism

Abhisek Mukherjee,[1]* Diego Morales-Scheihing,[1,2]* Natalia Salvadores,[1,3]* Ines Moreno-Gonzalez,[1] Cesar Gonzalez,[1] Kathleen Taylor-Presse,[1] Nicolas Mendez,[1] Mohammad Shahnawaz,[1] A. Osama Gaber,[4] Omaima M. Sabek,[4] Daniel W. Fraga,[4] and Claudio Soto[1,2]

[1]Mitchell Center for Alzheimer's Disease, Department of Neurology, John P. and Kathrine G. McGovern Medical School, University of Texas Medical School at Houston, Houston, TX
[2]Facultad de Medicina, Universidad de los Andes, Las Condes, Santiago, Chile
[3]Center for Integrative Biology, Universidad Mayor, Santiago, Chile
[4]Department of Surgery, Houston Methodist Hospital, Houston, TX

The Journal of Experimental Medicine

Although a large proportion of patients with type 2 diabetes (T2D) accumulate misfolded aggregates composed of the islet amyloid polypeptide (IAPP), its role in the disease is unknown. Here, we show that pancreatic IAPP aggregates can promote the misfolding and aggregation of endogenous IAPP in islet cultures obtained from transgenic mouse or healthy human pancreas. Islet homogenates immunodepleted with anti-IAPP–specific antibodies were not able to induce IAPP aggregation. Importantly, intraperitoneal inoculation of pancreatic homogenates containing IAPP aggregates into transgenic mice expressing human IAPP dramatically accelerates IAPP amyloid deposition, which was accompanied by clinical abnormalities typical of T2D, including hyperglycemia, impaired glucose tolerance, and a substantial reduction on β cell number and mass. Finally, induction of IAPP deposition and diabetic abnormalities were also induced in vivo by administration of IAPP aggregates prepared in vitro using pure, synthetic IAPP. Our findings suggest that some of the pathologic and clinical alterations of T2D might be transmissible through a similar mechanism by which prions propagate in prion diseases.

INTRODUCTION

Type 2 diabetes (T2D) mellitus is characterized by hyperglycemia, insulin resistance, defective insulin secretion, loss of β cell function and mass, and accumulation of amyloid in the islets of Langerhans (Stumvoll et al., 2005). The cause of T2D is not completely understood but is suspected to be related to a combination of lifestyle and genetic factors. The disease is due to insufficient insulin production from β cells in the setting of insulin resistance. However, not all people with insulin resistance develop diabetes (Polonsky, 2000) because an impairment of insulin secretion from pancreatic β cell dysfunction is required (Kahn, 2003). Dysfunction and loss of β cells has been associated with glucolipotoxicity (Poitout and Robertson, 2002; El-Assaad et al., 2003), islet cholesterol accumulation (Brunham et al., 2010), and islet inflammation (Donath and Shoelson, 2011). However, compelling evidence suggests that accumulation of amyloid aggregates in the islets of Langerhans might significantly contribute to β cell dysfunction and disease (Hull et al., 2004; Haataja et al., 2008; Jurgens et al., 2011; Mukherjee et al., 2015).

Islet amyloid deposits, composed predominantly of a misfolded and aggregated form of the islet amyloid polypeptide (IAPP), are observed in >90% of patients with T2D (Westermark, 1972; Clark et al., 1988; Betsholtz et al., 1989; Johnson et al., 1989). Autopsy studies in humans suggest that islet amyloid is associated with the loss of β cells mass (Clark et al., 1988). Mutations in the *IAPP* gene have been linked with an increased risk for T2D (Novials et al., 2001). Longitudinal studies in animals that spontaneously develop T2D (nonhuman primates and domestic cats) showed that detection of IAPP aggregates precedes β cell dysfunction and clinical signs of the disease (Howard, 1986; de Koning et al., 1993; Ma et al., 1998). Transgenic mice overexpressing human IAPP (hIAPP) develop islet amyloidosis and, associated to IAPP misfolding and oligomerization, the animals exhibit β cell loss, impaired insulin production, and fasting hyperglycemia (Janson et al., 1996). Overall, these results suggest an important role for IAPP misfolding and aggregation in islet pathology responsible for T2D. This finding does not contradict the widely accepted fact that insulin resistance is very important for T2D pathogenesis. Indeed, it is very likely that insulin resistance has a key role in IAPP aggregation because insulin resistance leads to an increase in IAPP production,

*A. Mukherjee, D. Morales-Scheihing, and N. Salvadores contributed equally to this paper.

Correspondence to Claudio Soto: Claudio.Soto@uth.tmc.edu

Abbreviations used: FTIR, Fourier-transformed infrared; hIAPP, human IAPP; IAPP, islet amyloid polypeptide; Mcc, microcin; PMD, protein misfolding disease; rpm, revolutions per minute; STZ, streptozotocin; T2D, type 2 diabetes; Tg, transgenic; ThS, thioflavin S; ThT, thioflavin T.

The Rockefeller University Press
J. Exp. Med. 2017 Vol. 214 No. 9 2591–2610
https://doi.org/10.1084/jem.20161134

since IAPP and insulin are cosecreted and subjected to the same regulatory mechanisms (Höppener et al., 2000). Thus, in prediabetic stages, obesity and insulin resistance may increase IAPP production, and it is very well established that an increase in protein concentration is one of the main factors leading to protein aggregation.

Accumulation of misfolded protein aggregates is not only present in T2D but also is the main feature of a group of diseases known as protein misfolding disorders (PMDs), including various neurodegenerative diseases, such as Alzheimer's disease, Parkinson's disease, amyotrophic lateral sclerosis, and prion disorders, as well as several systemic amyloidosis disease (Luheshi et al., 2008; Soto and Estrada, 2008). In PMDs, misfolding, aggregation, and accumulation of different proteins in distinct tissues leads to cellular damage, organ dysfunction, and disease. Among PMDs, prion diseases have the intriguing feature that the pathology can be transmitted by infection with the misfolded protein (Prusiner, 1998). Indeed, infectious prions are solely composed of preformed aggregates of misfolded prion protein, which transmit disease by seeding the aggregation of the endogenous prion protein, resulting in the accumulation of large quantities of these toxic aggregates in the brain (Prusiner, 1998; Soto et al., 2006). It is thought that the ability of misfolded prion protein to serve as a nucleus for the misfolding and aggregation of the host prion protein is the key property responsible for prion replication and infectivity (Soto et al., 2006; Soto, 2012). Interestingly, the formation of misfolded aggregates in T2D, as well as in all other PMDs, follows a seeding/nucleation mechanism, similar to the process of prion replication, in which preformed polymers seed the aggregation of the monomeric endogenous protein (Soto et al., 2006; Soto, 2012). The similarities between the molecular mechanism of prion propagation and the process of protein misfolding and aggregation in PMDs, suggest that misfolded aggregates have an inherent ability to be transmissible (Soto et al., 2006; Soto, 2012). Indeed, a series of recent, exciting studies have shown that the pathologic hallmarks of various PMDs, including Alzheimer's, Parkinson's, Huntington's diseases, and some forms of systemic amyloidosis, can be induced under experimental conditions by administration of tissue homogenates carrying the respective misfolded proteins (Xing et al., 2001; Lundmark et al., 2002; Meyer-Luehmann et al., 2006; Clavaguera et al., 2009; Ren et al., 2009; Eisele et al., 2010; Grad et al., 2011; Luk et al., 2012; Morales et al., 2012; Mougenot et al., 2012; Stöhr et al., 2012; Iba et al., 2013).

We hypothesized that islet IAPP aggregation and associated diabetic pathology could be induced by seeding with preformed IAPP aggregates through a prion-like mechanism. To test that hypothesis, we performed ex vivo studies using isolated islets cultures and in vivo experiments in a transgenic (Tg) mouse model overexpressing hIAPP. The results indicate that IAPP aggregation can be promoted by administration of pancreatic tissue homogenates containing preformed IAPP aggregates. The pathologic induction did not occur when the aggregates were removed with antibodies specific to IAPP. Interestingly, associated to IAPP accumulation, animals developed some of the typical clinical abnormalities of T2D, including hyperglycemia, impaired glucose tolerance, and loss of β cells. Finally, islet pathology and associated clinical alterations were induced by administration of in vitro, prepared IAPP aggregates made from pure, synthetic hIAPP. Our findings suggest that misfolded IAPP can self-propagate in a manner reminiscent of infectious prions and that IAPP accumulation may have an important role in islet dysfunction in T2D.

RESULTS

Pancreatic IAPP aggregates induce endogenous IAPP deposition in cultures from Tg mice and human islets

To begin evaluating whether islet amyloid pathology might be transmissible, we performed studies in islets isolated from Tg mice that overexpress hIAPP (Tg-hIAPP). It has been shown that mouse IAPP is not amyloidogenic and does not accumulate as aggregates in the pancreas (Westermark et al., 1990; Janson et al., 1999; Ritzel and Butler, 2003). Male homozygous mice for hIAPP develop T2D-like clinical and pathologic alterations, including hyperglycemia, reduced insulin secretion, IAPP amyloid deposits, and β cell loss (Janson et al., 1996). IAPP aggregation starts as small, intracellular aggregates and later becomes accumulated as massive, extracellular deposits over time. 12-mo-old Tg mice displayed extensive islet pathology and overt signs of T2D, including massive amyloid deposits, impaired insulin production (Fig. 1) and severe hyperglycemia (>360 mg/dl fasting blood glucose). Age-matched, non-Tg mice of the same background, which did not have any detectable IAPP aggregates (Fig. 1), were used as controls.

Isolated islets from 3-wk-old Tg-hIAPP, which do not exhibit IAPP aggregates at that age (Janson et al., 1996), were cultured in the presence of 1% or 0.1% islets extracts from old Tg or WT mice for 7 d under standard conditions, including a glucose concentration of 11 mM in the medium to reduce glucotoxicity and spontaneous aggregation of the protein (Zraika et al., 2007). Those doses were chosen in analogy with the prion field, in which it is very common to observe that 1% and 0.1% tissue homogenate containing prion protein aggregates is able to induce pathological changes both in cell culture experiments and in in vivo animal models. As shown in Fig. 2 A, treatment with 1% islet homogenate from diabetic mice leads to punctated accumulation of thioflavin S (ThS)–positive amyloid aggregates in cultured islets. In contrast, islets untreated or treated with nondiabetic, WT islet homogenates did not show any significant accumulation of amyloid. To rule out that the staining was coming from the aggregates present in the inoculum, cultured islets from WT animals, which do not express hIAPP, were incubated with the same amount of old Tg islet homogenate. The results showed only a small amount of staining that was not substantially higher than untreated islets (Fig. 2 A, bottom). The amyloid load was quantitatively analyzed by measuring the

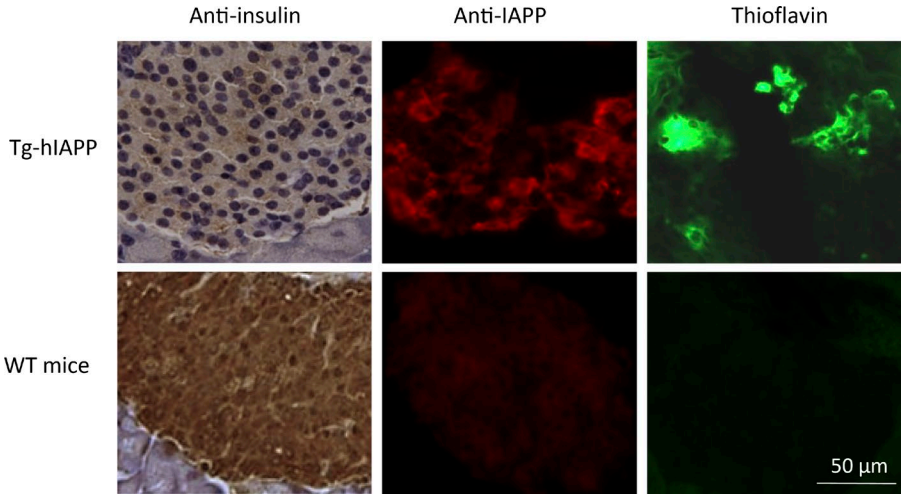

Figure 1. **Characterization of the pancreas tissue used as inoculum in our studies.** Pancreas from a 12-mo-old, male, Tg-hIAPP mouse exhibiting overt signs of diabetes (blood glucose >360 mg/dl) as well as an age-matched WT mice used as control were extracted and analyzed histologically by immunohistochemistry using anti-IAPP and anti-insulin antibodies and ThS staining. Images display staining of representative sections.

percentage of ThS-positive area to total islet area delimited by DAPI staining (Fig. 2 B). These results suggest that material containing aggregated IAPP seeds can induce the aggregation and deposition of new IAPP amyloid in cultured islets and that the formation of new amyloid deposits depends on the expression of endogenous hIAPP in the islets.

The previous experiment was performed using isolated islets from Tg mice that overexpress hIAPP and thus are genetically predisposed to accumulate IAPP aggregates. To analyze the relevance of these results in a more-natural situation in humans, we performed an ex vivo experiment using islets isolated postmortem from human subjects nonaffected by T2D. In those islets, hIAPP is expressed at physiological levels from the endogenous promoter. Islets from nondiabetic human subjects exposed to islet homogenate from diabetic Tg-hIAPP mouse harboring extensive hIAPP aggregates developed substantial accumulations of ThS-positive amyloid deposits (Fig. 2 C). The load of IAPP aggregates in islets treated with old Tg-hIAPP islet homogenate was significantly greater than that of the control groups, including untreated human islets and those exposed to the same concentration of WT islet extracts lacking IAPP aggregates (Fig. 2 D). These data clearly show that exposure to islet extracts containing IAPP seeds induces IAPP aggregation in healthy human islets in culture. To show that IAPP aggregates are the active principle in seeding IAPP deposition, we included a group treated with islet extracts that was specifically immunodepleted of IAPP. hIAPP was depleted from the islet homogenate of diabetic Tg-hIAPP mice, using a cocktail of sequence-specific and conformational antibodies. The efficiency of immunodepletion was confirmed by Western blot using anti-IAPP–specific antibodies (Fig. 2 D, inset). The results showed that the IAPP immunodepleted material was unable to induce aggregation in islets isolated from healthy human subjects (Fig. 2, C and D).

Transmission of IAPP aggregates in vivo

To study the ability of IAPP aggregates to induce IAPP misfolding and other pathologic alterations typical of T2D in vivo, we performed experiments using Tg-hIAPP mice. All in vivo experiments, including controls and inocula, were performed with male Tg mice. Groups of 3-wk-old, Tg-hIAPP, homozygous male mice were inoculated with a single i.p. injection of 100 µl of 10% pancreas homogenate. The inoculum was obtained from 12-mo-old Tg mice bearing extensive islet pathology and overt signs of T2D, including massive amyloid deposits (Fig. 1) and high levels of glucose in blood (>360 mg/dl in fasting condition). As controls, groups of male Tg mice were injected with pancreas homogenate from age-matched non-Tg mice that did not have any detectable IAPP aggregates (Fig. 1). Groups of five animals in each condition were sacrificed at 5, 8, 10, and 20 wk of age, and pancreata were analyzed by histology. Tg-hIAPP mice inoculated with Tg pancreas homogenate containing IAPP aggregates (hereafter termed the Tg/Tg group) exhibited punctate staining with anti-IAPP antibody (Fig. 3 A) and ThS (Fig. 3 B), starting at ∼8 wk of age. Amyloid staining increased over time, and by 20 wk of age, it was extensive, exhibiting the typical morphology of amyloid deposits (Fig. 3, A and B). Conversely, Tg-hIAPP mice inoculated with WT pancreas homogenate (hereafter referred to as the Tg/WT group) only began to show small IAPP aggregates at around 20 wk of age (Fig. 3, A and B), in a manner similar to untreated Tg mice. Staining with anti-IAPP antibody colocalized with ThS (Fig. 3 C), indicating that those deposits are amyloid aggregates composed predominantly of IAPP. To make sure that amyloid aggregates were located inside the islets of Langerhans, all sections were simultaneously stained with ThS (green) and anti-insulin antibody (red). Fig. 3 D shows one representative image of that costaining for an animal of the group treated with Tg-hIAPP pancreas homogenate and sacrificed at 20 wk old, depicting the ThS signal in association with β cells. Image analysis studies of the IAPP staining (Fig. 3 A) show that both the percentage of islets containing IAPP aggregates (Fig. 3 E) and the load of IAPP deposits (Fig. 3 F) in the Tg/Tg group of mice progressively increased with age. The stepwise increase in amyloid deposition (both in size and number of

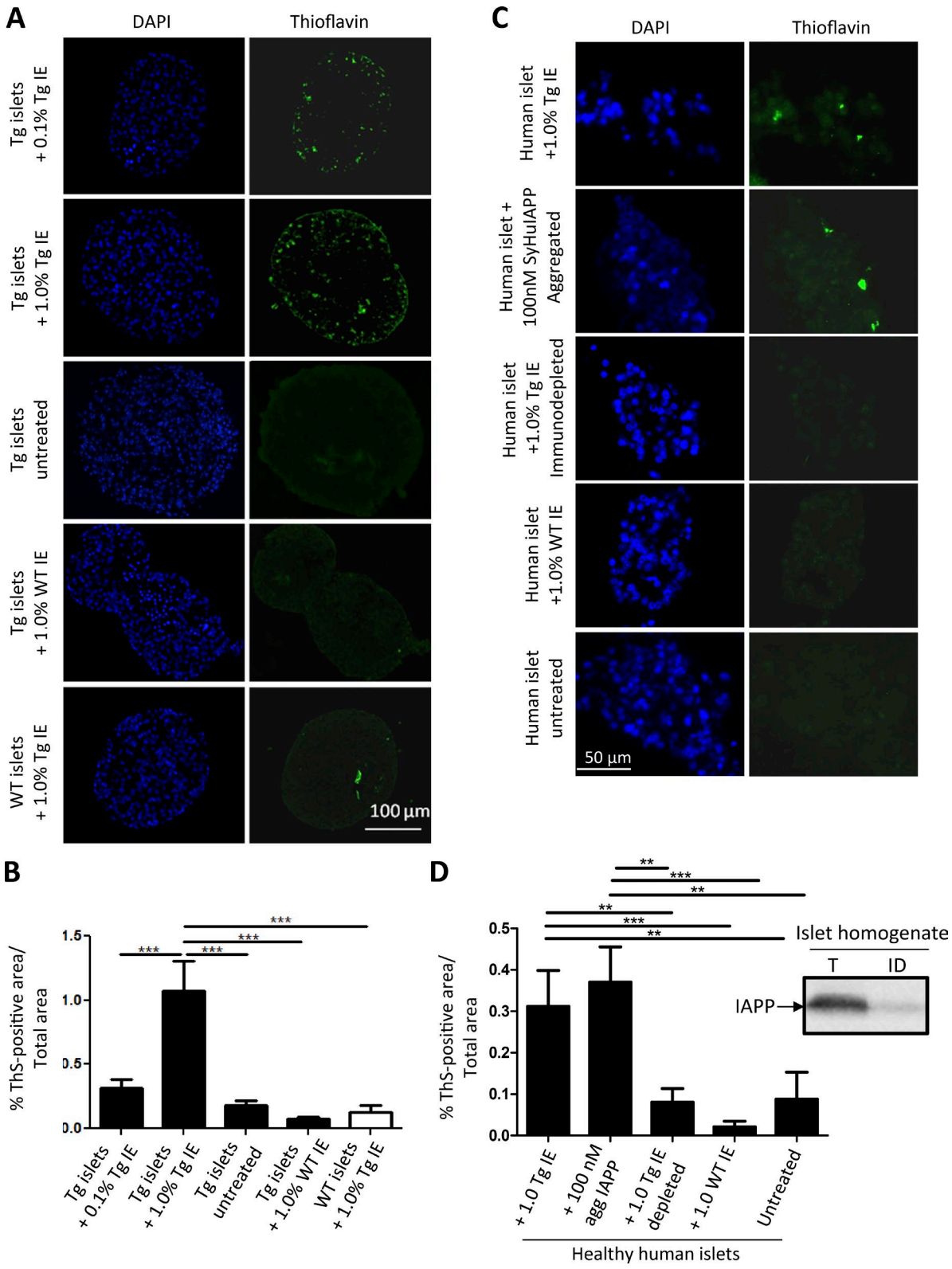

Figure 2. **Islet homogenate from aged Tg-hIAPP mice induces IAPP deposition in isolated islet cultures from either Tg mice or healthy humans.** (A) Isolated islets from 3-wk-old, female, Tg-hIAPP mice were cultured in presence of different concentrations of islet extracts (IE) from old Tg-hIAPP mice, with overt diabetic pathology and age-matched WT mice. Representative images of islets, after diverse treatments, characterized by DAPI staining (blue) and by presence of amyloid by ThS amyloid staining (green). (B) The amyloid load present in the islets was quantified by measuring ThS-positive area/total

deposits) with time suggests that the IAPP deposits detected were not coming from the injected material, but rather, from new deposition of endogenous, misfolded IAPP aggregates. That conclusion was further supported by the results of an experiment in which the same old Tg pancreatic homogenate used previously was inoculated into WT, non-Tg mice of the same background. Those animals did not exhibit any detectable IAPP aggregates (Fig. S1 A). The extent of IAPP amyloid deposition in Tg/Tg mice was, at all time points, significantly higher than the staining observed in Tg-hIAPP animals inoculated with control pancreas homogenate (Fig. 3 F). Our findings clearly demonstrate that administration of material containing IAPP aggregates accelerates endogenous IAPP misfolding and aggregation. To rule out that the induction observed was due to other diabetic-associated alterations in the pancreas, we performed a control experiment in which we injected Tg-hIAPP mice with pancreas homogenate from a diabetic model not associated with IAPP aggregation. For that purpose, we used a streptozotocin (STZ) model of diabetes, which is widely used in the field to produce destruction of β cells and hyperglycemia (Wilson and Leiter, 1990). Treatment of Tg-hIAPP mice with that material did not produce any effect in terms of inducing IAPP aggregation, as compared with control, untreated Tg mice (Fig. S2). These results strongly indicate that the effect observed was dependent on the presence of IAPP aggregates acting as seeds to induce the pathology by a prion-like mechanism and was not due to other changes associated with diabetic conditions.

Induction of IAPP aggregation in vivo leads to T2D-like abnormalities

To investigate whether induction of IAPP aggregation leads to some of the clinical alterations typically observed in patients with T2D, we measured fasting blood glucose at different times after inoculation in the same animals used for IAPP histological analysis shown above. Fasting blood glucose level became significantly higher in animals injected with Tg-hIAPP pancreas homogenate containing IAPP aggregates, as early as 8 wk compared with mice treated with WT pancreas extracts (Fig. 4 A). Glucose levels continued increasing in the Tg/Tg groups throughout the course of the experiment. In fact, by 20 wk of age >70% of the animals in this group developed hyperglycemia, defined as a blood glucose concentration >250 mg/dL (Fig. 4 B). In contrast, none of the Tg animals inoculated with normal pancreas homogenates showed elevated blood glucose up to 20 wk of age (Fig. 4, A and B). To test impairment of glucose metabolism, we performed a glucose tolerance test in animals at the age of 16 wk. Animals fasted for 16 h were injected with 1 g/kg body weight of glucose i.p., and blood glucose level was monitored subsequently at different time intervals. Tg-hIAPP mice injected with pancreas homogenates containing IAPP aggregates reached a higher level of blood glucose compared with control animals (Fig. 4 C). Moreover, those animals took longer to decrease glucose in blood, which did not return to basal levels even 120 min after glucose administration (Fig. 4 C). The differences were also evident by measuring the area under the curve in the graph (Fig. 4 C, inset). To evaluate islet dysfunction and β cells damage, we studied islet morphology by staining α-, β-, and δ cells using anti-glucagon, anti-insulin, and anti-somatostatin antibodies, respectively (Fig. 4 D). The results showed that Tg-hIAPP injected with pancreatic homogenate containing IAPP aggregates (the Tg/Tg group) exhibited an altered islet morphology characterized by the appearance of α- and δ-cells in the center of the islets, compared with the classical pattern in mice (observed in Tg/WT), in which these cells are mostly confined to the periphery of the islets (Brissova et al., 2005). The presence of α- and δ-cells inside the islet typically occurs because of the death of a massive numbers of β cells (Janson et al., 1996; Kharouta et al., 2009). The area of the islets occupied by β cells was significantly reduced in the Tg/Tg group, as compared with control mice. Indeed, the number of β cells/mm^2 of pancreas in the Tg/Tg group was on average >60% lower in comparison with Tg/WT mice (Fig. 4 E). Further analysis revealed that the mice in Tg/Tg group, which developed severe hyperglycemia, lost >75% of their β cells compared with WT mice of the same strain and similar age. It has been reported that in a Tg rodent (rat) model expressing hIAPP, diabetes onset coincides with a ∼60% deficit in β cell mass (Butler et al., 2004), which resembles the ∼70% loss of β cell mass observed in patients with T2D (Butler et al., 2003). Thus, our results strongly suggest that substantial loss of β cells is the likely cause of the diabetic phenotype in the animals treated with IAPP aggregate-containing materials. Our findings demonstrate that induction of IAPP misfolding and aggregation by administration of preformed IAPP-aggregated seeds leads to the development of marked T2D-like pathology, including severe hyperglycemia, impaired glucose homeostasis, loss of β cells, and changes in islets morphology. These abnormali-

islet area. The values correspond to means ± SE of 5–20 islets analyzed per condition. Data were analyzed by one-way ANOVA, and differences were highly significant ($P < 0.0001$). Individual differences were evaluated by Tukey's multiple comparison posttest (***, $P < 0.001$). (C) Human islets, isolated postmortem from nondiabetic individuals, were treated with 1% islet homogenate from old Tg-hIAPP mice, WT control islet homogenates, or old Tg-hIAPP immunodepleted using a cocktail of sequence and conformational antibodies. In addition, human islets were incubated with 100 nM synthetic IAPP aggregates using the conditions described in Fig. 5. After 10 d, islets were fixed and stained with DAPI (blue) and ThS (green). Representative pictures from each condition. (D) The amyloid present in islets was quantified by measuring the percentage of ThS-positive area/total islet area. On average, 27 islets were analyzed per condition, and data correspond to mean ± SE. (Inset) Amount of IAPP signal present in the extracts of islet homogenates before and after immunodepletion, as measured by Western blot. Data were analyzed by Kruskal–Wallis test, and treatment differences were highly significant ($P < 0.0001$). Individual differences were evaluated by Dunn's multiple comparison test. **, $P < 0.01$; ***, $P < 0.001$.

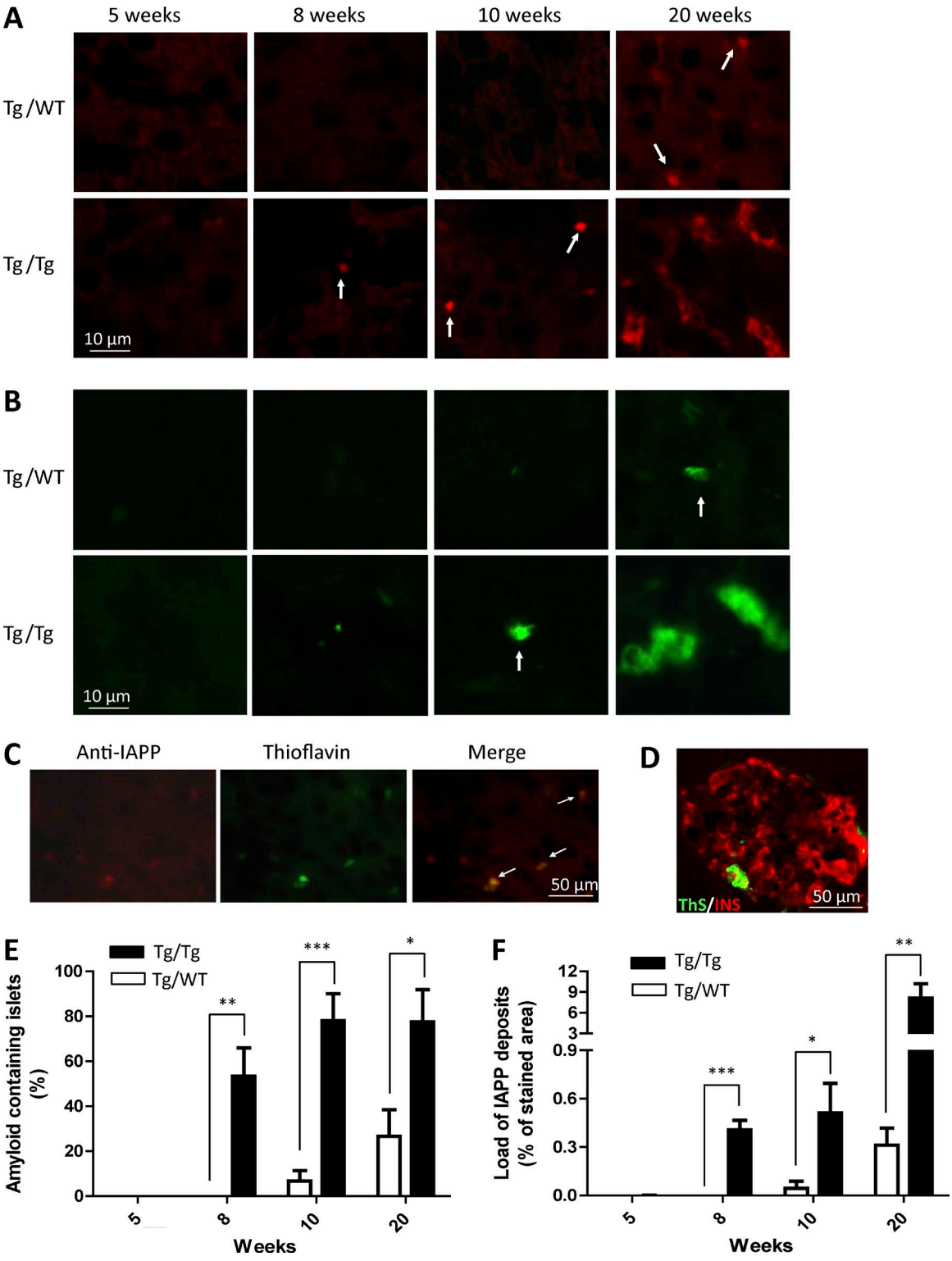

Figure 3. **Inoculation with old Tg-hIAPP pancreas homogenate accelerates IAPP misfolding and aggregation.** (See also Figs. S1 and S2.) Groups of male Tg-hIAPP mice were injected i.p. at 3 wk of age with 10% pancreas homogenate from either 12-mo-old, male, IAPP Tg mice bearing substantial islet amyloid aggregates (as shown in Fig. 1) or from age-matched, male, WT mice not expressing hIAPP. Groups of three to sixmice were sacrificed 2, 5, 7, and 17 wk after inoculation, when they reached 5, 8, 10, and 20 wk of age, respectively. Appearance of IAPP aggregates was assessed by histologic studies using anti-IAPP antibody (A) or the amyloid-binding dye ThS (B). (A and B) Figures correspond to representative pictures of the five animals studied, except in the case of the animals treated with WT pancreas homogenate and sacrificed at 10 wk old; in which, 2 animals died of unrelated reasons. Arrows highlight

ties were not observed during the time of our experiments in Tg-hIAPP untreated mice or mice injected with pancreas homogenate without IAPP aggregates.

Ex vivo induction of IAPP accumulation by synthetic IAPP aggregates

The interpretation of the findings described above is that IAPP aggregates present in the inoculated material act in a prion-like manner to seed aggregation of endogenous IAPP. However, because the material injected has many other components, we cannot completely rule out that another molecule could be implicated in the pathologic induction. To study whether IAPP aggregates were the active principle in inducing pancreatic changes, transmission experiments were performed using pure protein aggregates prepared from synthetic hIAPP in vitro. Amyloid formation was followed by a thioflavin T (ThT) binding assay (Fig. S3 A), which is a widely used procedure for monitoring amyloidosis and is based on the specific interaction of ThT with amyloid structures (Levine, 1993). Enriched β sheet content in IAPP aggregates was confirmed by Fourier-transformed infrared (FTIR) spectroscopy. Indeed, although soluble IAPP has FTIR spectra with a maximum absorption of ∼1,654 cm^{-1}, consistent with a predominance of α-helix/random coil structure (Yang et al., 2015), aggregated IAPP exhibited a maximum absorption of ∼1,638 cm^{-1}, indicating that β sheets are the predominant structure (Fig. S3 B). Fibrillar morphology was confirmed by transmission electron microscopy after negative staining (Fig. S3 C). As expected, preformed IAPP aggregates were able to seed IAPP aggregation in vitro (Fig. S3 D).

First, we tested the seeding potential of the synthetic aggregates in the ex vivo model using islet cultures. Islets isolated from 3 wk-old Tg-hIAPP mice were treated with different concentrations of synthetic IAPP-aggregated seeds for 10 d. As before, islet amyloid formation was analyzed by measuring the ThS-positive area. Islets treated with 10, 50, and 100 nM synthetic IAPP aggregates accumulated a progressively higher level of amyloid compared with untreated islets (Fig. 5). The rationale for the doses selected was to mimic the putative quantities that islets might be exposed through blood irrigation. Serum IAPP levels in normal individuals range from 1 to 90 pM (Paulsson et al., 2014). In prediabetes or diabetic conditions, the serum IAPP levels may be substantially higher because insulin resistance promotes greater expression of insulin and IAPP. Because the islets are continuously perfused by blood, it is likely that they may receive much larger quantities of blood-borne IAPP aggregates over a long time. In isolated islets, it is not possible to recapitulate multiple exposures because the islets do not survive very long in culture. Therefore, we have used concentrations of IAPP aggregates in the nanomolar range in our ex vivo studies to mimic the possible physiologic conditions within the technical limitations of the experiments.

Treating islets with 100 nM nonaggregated, monomeric IAPP did not produce any significant increase in IAPP amyloid accumulation, indicating that the effect was dependent on the aggregated conformation of the material added (Fig. 5). To test the specificity of the effect, we also treated islets with aggregates coming from other disease-associated and functional amyloid proteins. For that purpose, we used aggregates of the Tau protein, implicated in Alzheimer's disease, as well as the bacterial amyloid protein microcin (Mcc). For the Tau protein, we used the K18 fragment containing four microtubule binding repeats, which is considered the core of the Tau amyloid fibril and is often used as a model of Tau protein for aggregation experiments (Siddiqua and Margittai, 2010; Shammas et al., 2015). Mcc is a small–molecular-weight bacteriotoxin, with activity regulated in vivo by aggregation into amyloid fibrils at the stationary phase of the bacterial culture (Bieler et al., 2005; Shahnawaz et al., 2017). Tau and Mcc were induced to form amyloid aggregates by incubation in buffer, and amyloid fibril formation was characterized by ThT and transmission electron microscopy (Fig. S4). Treatment of islets with Tau and Mcc aggregates did not increase IAPP deposition in the islets cultures. These results indicated that, under our experimental conditions, other amyloidogenic proteins do not induce significant accumulation of IAPP compared with amyloid aggregates composed of IAPP. As controls, we also treated islets from WT mice, which do not express hIAPP, with 100 nM aggregated IAPP; no significant accumulation of IAPP amyloid was observed in that experiment (Fig. 5), suggesting that IAPP accumulation in Tg islets was composed of new deposition of endogenous IAPP nucleated by the exogenously added synthetic aggregates. Similar results were obtained when human islets were treated with synthetic IAPP aggregates (Fig. 2, C and D).

small punctate deposits. (C) Slides were stained simultaneously with anti-IAPP antibody and ThS and colocalization of the staining analyzed. The picture corresponds to an animal of the Tg-hIAPP inoculated group sacrificed at 10 wk old. Arrows in the merged image point to the deposits in which colocalization was observed. (D) Double-staining with ThS (green) and anti-insulin antibody (red). The picture corresponds to a representative image of one animal treated with Tg-hIAPP pancreas homogenate and sacrificed at 20 wk old. Image analysis of the immunohistochemical studies displayed in A (staining with an anti-IAPP antibody) was performed to estimate the percentage of islets containing amyloid deposits (E) and the load of IAPP aggregates (F), calculated as the percentage of the stained area compared with the total islet area. The values correspond to the mean ± SE of the results obtained for the three to six animals used per each group. (E and F) Black bars represent the animals inoculated with old Tg-hIAPP pancreas homogenate, and white bars correspond to the controls injected with WT pancreas. The data were statistically analyzed by two-way ANOVA using age and source of inoculation as the variables. In both cases, the overall results were statistically significant ($P < 0.001$). Individual differences between Tg/Tg and Tg/WT animals were studied by the Bonferroni posttest. *, $P < 0.05$; **, $P < 0.01$; ***, $P < 0.001$.

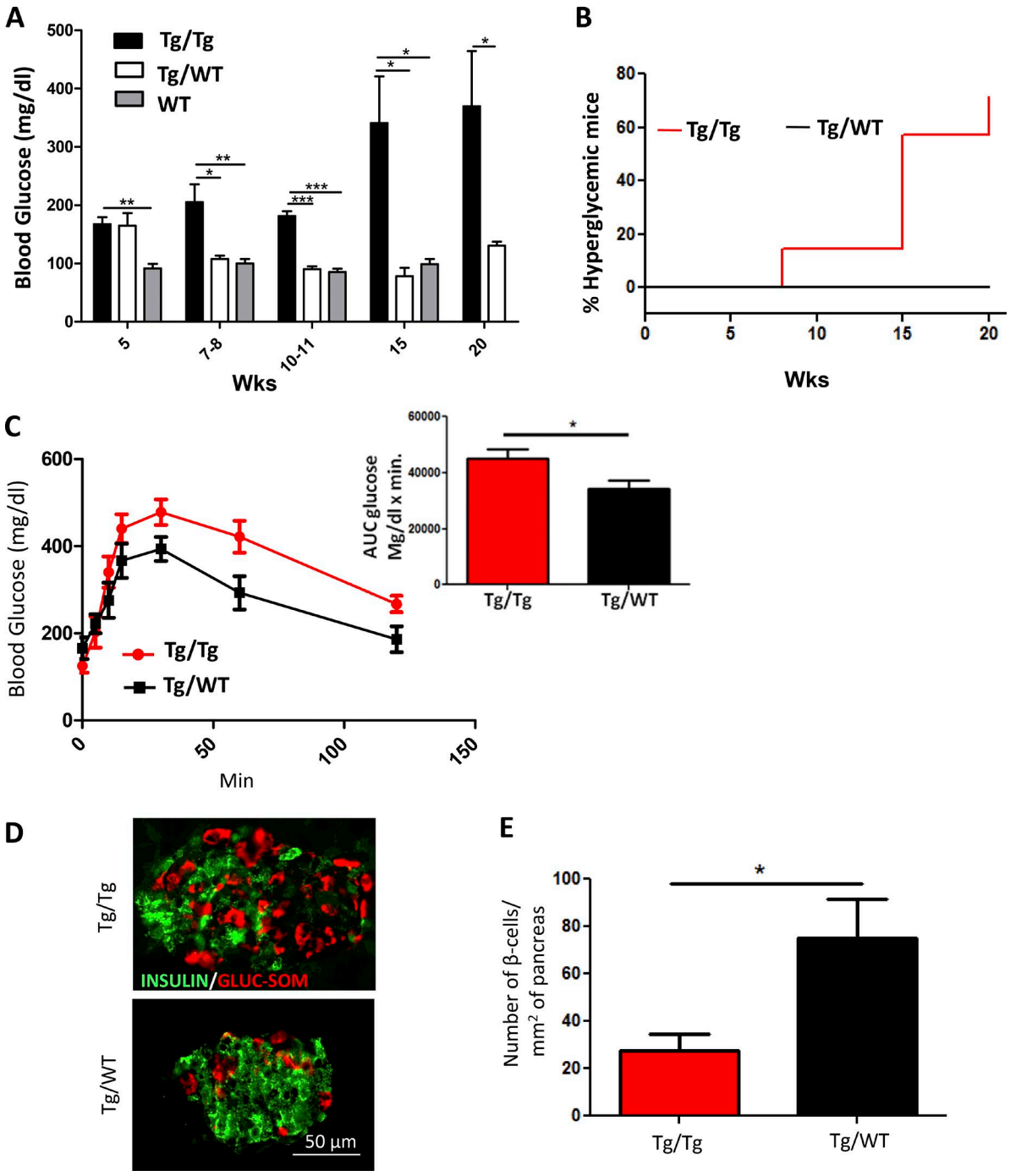

Figure 4. **Inoculation with old Tg-hIAPP pancreas homogenate induces clinical abnormalities typical of T2D.** (See also Figs. S1 and S2.) (A) Hyperglycemia was measured over time by the fasting blood glucose concentration. The values correspond to the mean ± SE of the results obtained from five to seven animals in each group. Black bars represent the Tg-hIAPP mice inoculated with old Tg-hIAPP pancreas homogenate, and white bars the controls injected with WT pancreas homogenate. For comparison, the blood glycemia of WT, untreated animals is shown (gray bars). The data were statistically analyzed by two-way ANOVA using age and source of inoculation as the variables. The analysis shows that the increase in glucose concentration in the Tg/Tg group was highly significant ($P < 0.001$). Individual differences between groups on different days were analyzed by one-way ANOVA followed by the Tukey's multiple comparison posttest. *, $P < 0.05$; **, $P < 0.01$; ***, $P < 0.001$. (B) Inoculation with diabetic pancreas homogenate produced severe hyperglycemia (>250 mg/dL) in a portion of the animals. The percentage of hyperglycemic animals increased progressively with time after inoculation of Tg pancreas extracts, whereas up to 20 wk of age, no animals of the Tg/WT group reached the threshold to be considered hyperglycemic. The differences were statistically significant ($P = 0.02$) as analyzed by the log-rank (Mantel–Cox) test. (C) To evaluate impairment in glucose tolerance, the i.p. glucose tolerance test was performed in 16-wk-old, Tg-hIAPP mice inoculated with pancreas extracts from old Tg-hIAPP (red line) as compared with Tg-hIAPP mice inoculated with

In vivo induction of IAPP deposition and associated diabetic abnormalities by synthetic IAPP aggregates

Next, we investigated whether injection of pure, synthetic IAPP aggregates was able to induce IAPP deposition and associated diabetic abnormalities in vivo. These experiments were performed in a manner similar to the studies described in Fig. 3. Groups of 3-wk-old, Tg-hIAPP, homozygous male mice were given a single i.p. injection of 100 μl of 50-μM synthetic IAPP aggregates. As controls, animals were injected with the same concentration of nonaggregated IAPP monomers, and another group was treated with PBS. The results clearly showed that injection of synthetic IAPP aggregates induced a marked increase in the accumulation of IAPP- and ThS-positive deposits in the pancreatic islets of animals sacrificed 13 wk after inoculation (16 wk old; Fig. 6 A). As before, amyloid staining was located inside the islets in association with β cells, as demonstrated by costaining between ThS and insulin (Fig. 6 B). Quantification of aggregates by image analysis of slides stained with anti-IAPP antibodies (Fig. 6 C) and ThS (Fig. 6 D) showed a twofold greater burden of IAPP deposits in mice inoculated with synthetic aggregates, as compared with the PBS-treated controls and the animals injected with nonaggregated IAPP. Injection of IAPP aggregates into WT mice did not show a significant amount of staining, indicating that the aggregates observed in the experimental group were not composed solely of the inoculated material.

To investigate whether inoculation of pure, synthetic IAPP aggregates can accelerate clinical alterations typical of T2D, we measured fasting blood glucose concentrations and the integrity of islet morphology. Fasting glycemia was measured periodically in Tg-hIAPP mice treated with synthetic IAPP aggregates or PBS as well as in WT mice injected with the same preparation of synthetic aggregates (Fig. 7 A). Starting at around 9 wk old, Tg mice inoculated with synthetic aggregates showed clearly higher blood glucose concentrations than control animals had, and the concentrations kept increasing until animals were sacrificed for histologic analysis. Indeed, the percentage of severely hyperglycemic animals was clearly higher in the group of Tg-hIAPP treated with synthetic aggregates, reaching 36% at 16 wk old, whereas none of the controls showed high glycemia at that time (Fig. 7 B). As before, abnormalities of islet morphology and β cells loss were studied by staining α-, β-, and δ-cells using anti-glucagon, anti-insulin, and anti-somatostatin antibodies, respectively (Fig. 7 C). In the group of mice treated with synthetic IAPP aggregates, we observed a substantial reduction in the area of islets occupied by β cells as compared with controls untreated or treated with the same concentration of nonaggregated IAPP (Fig. 7 D).

IAPP aggregates do not produce toxicity or IAPP accumulation in nonpancreatic tissues

Our previous results showed that administration of IAPP aggregate-containing material resulted in significant accumulation of IAPP in the recipient Tg-hIAPP mice, starting at ~8 wk (Fig. 3, A, B, E, and F). To test whether the inocula produced any other type of toxicity in the recipient mice, a group of 4-wk-old, male, Tg-hIAPP mice was inoculated with a single i.p. injection of 100 μl of 10% pancreas homogenate. The inoculum was obtained from old diabetic mice (fasting plasma glucose >360 mg/dl), following a similar experimental paradigm as presented in Fig. 3. Another group of 4-wk-old, male, Tg-hIAPP mice was also i.p inoculated with 100 μl of 50 μM synthetic IAPP aggregates, prepared in vitro. As a control, a group of age- and gender-matched Tg-hIAPP mice were i.p inoculated with buffer (PBS). To measure signs of general toxicity, body weights of recipient Tg-hIAPP mice were measured at 8 wk of age. No significant difference in body weight was observed in the groups treated with diabetic pancreas homogenate, containing IAPP aggregates or synthetic IAPP aggregates, prepared in vitro, compared with Tg-hIAPP mice injected with buffer (Fig. 8 A). To further assess signs of toxicity, we harvested major organs, including liver, kidney, spleen, heart, pancreas, and brain and analyzed the organ weight tobody weight ratio, a standard pharmacological procedure to test major organ toxicity. The results indicated that the administration of diabetic pancreas homogenate, containing IAPP aggregates or synthetic IAPP aggregates, prepared in vitro did not produce any significant changes in the weight of major organs, compared with the controls treated with buffer (Fig. 8 B). The fact that the pancreas weight did not change either, despite the animals showing evidence of diabetes, is not surprising because only ~1% of pancreas weight corresponds to islets of Langerhans. To analyze whether the administration of the inocula lead to pathologic accumulation of IAPP in any other major tissues, we analyzed sections of different tissues, stained with anti-IAPP antibody for a 250-μm range. We could not find accumulation of IAPP in any of the tissues tested, except for the pancreas (Fig. 8 C). Furthermore, we analyzed sections from tissues directly associated with glucose homeostasis (liver and skeletal muscle), stained with hematoxylin and eosin, over a range of 250 μm. Our analysis revealed no gross morphological abnormalities in the groups treated with

PBS (black line). The graph shows plasma glucose concentrations during the test after 16 h fasting. Area under the curve (AUC) was calculated using the trapezoidal rule (inset), and the values corresponds to means ± SE from five animals/group. The data were statistically analyzed by unpaired two-tailed *t* test (P = 0.0373). (D) The morphology of islets and the presence of different cell types was measured in different groups of mice at 20 wk old by staining with anti-insulin (green) to detect β cells, anti-glucagon, and anti-somatostatin antibodies (combined, red) to detect α- and δ-cells, respectively. The figure shows representative images of the islets from the Tg/Tg and Tg/WT mice. Image analysis of stained islets enabled us to calculate the number of β cells/mm^2 of pancreas area (E). Data correspond to the mean ± SE, and results were analyzed by unpaired two-tailed *t* test (*, P = 0.0234).

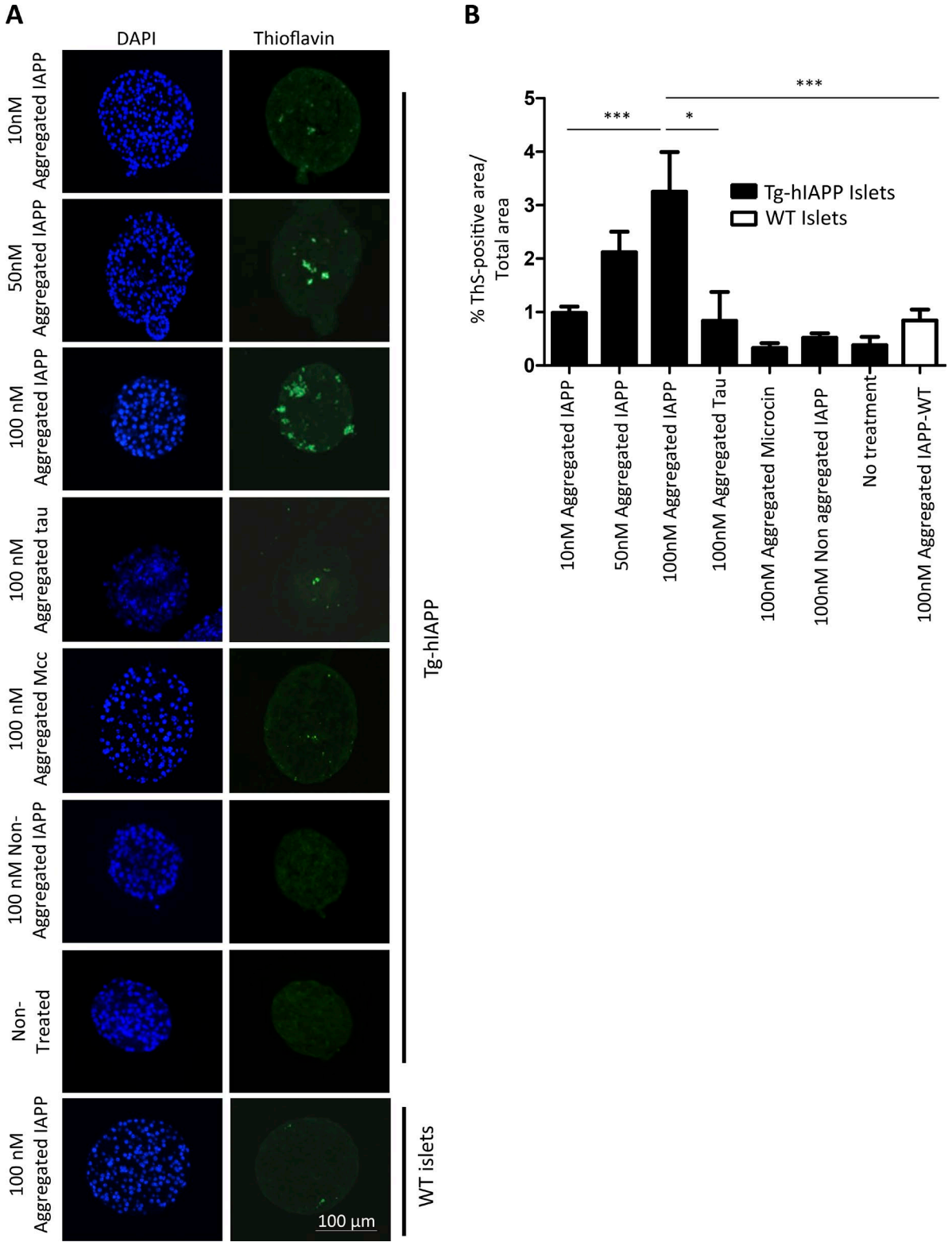

Figure 5. **Induction of IAPP amyloid deposition in islets by incubation with synthetic IAPP aggregates.** (See also Figs. S3 and S4.) (A) Isolated islets from 3-wk-old, female, Tg-hIAPP mice were cultured in presence of different concentrations of IAPP aggregates prepared in vitro from synthetic IAPP, as well as controls treated with other amyloidogenic proteins, including the Alzheimer's disease–associated protein Tau (the K18 fragment) and the bacterial amyloid Mcc. Representative images of islets after diverse treatments, characterized by DAPI staining (blue) and the presence of amyloid by ThS amyloid

IAPP aggregate-containing material, compared with buffer-treated controls (Fig. 8 D).

DISCUSSION

Although several environmental and genetic factors have been shown to contribute to the risk of T2D (e.g., obesity, inactivity, and aging), the origin of this disease is still not completely understood (Stumvoll et al., 2005). One of the hallmark abnormalities in T2D is the extensive dysfunction and loss of β cells (Kahn, 2003; Nyalakonda et al., 2010). The cause of β cell damage in T2D is currently unknown, but compelling evidence implicates the formation and accumulation of IAPP misfolded aggregates in the pancreas (Hull et al., 2004; Haataja et al., 2008; Jurgens et al., 2011; Mukherjee et al., 2015), in a manner similar to the way protein aggregates have been shown to be causative agents in a variety of chronic and progressive PMDs (Soto, 2003). Extensive work has been performed to understand the mechanisms of β cell loss induced by the formation and accumulation of IAPP misfolded aggregates. We have recently summarized those mechanisms (Mukherjee et al., 2015), which include membrane disruption, mitochondrial damage, endoplasmic reticulum stress, impairment of the ubiquitin proteasome system and autophagy, oxidative stress, and induction of inflammation. However, it is still unclear which of those various pathways are the most relevant during the disease.

A series of exciting recent studies suggested that the process of protein misfolding and aggregation implicated in various PMDs can be transmitted by administration of preformed, misfolded protein aggregates, in a way reminiscent of the transmission of prion diseases by infectious prions (Prusiner, 2012; Soto, 2012; Jucker and Walker, 2013). Our current study aimed to provide proof-of-concept for this phenomenon in diabetes, and for that reason, we used the models and methodologies traditionally used in the prion field to demonstrate the transmission process. These models include in vitro experiments with purified recombinant or synthetic proteins, cell culture experiments, and infectivity studies with Tg mice expressing the appropriate form of the protein. The findings obtained in our study not only extend the concept of prion-like transmission to the most prevalent disease of the PMD group but also show that transmission of protein misfolding leads to bona fide disease phenotypes. This is a subject of great importance, because, in most previous studies, the transmission of the pathologic misfolded aggregates did not induce the disease phenotype, raising a debate about whether seeding of protein misfolding is equivalent to disease transmission by infectious proteinaceous agents (Guest et al., 2011; Schmidt et al., 2012; Fernández-Borges et al., 2013; Piccardo et al., 2013; Walsh and Selkoe, 2016). Our ex vivo and in vivo results suggest that misfolded IAPP aggregates deposited in pancreatic tissue during the development of T2D can act as seeds to spread that process throughout the pancreatic islets or, under defined experimental conditions, even to other individuals. The results obtained in the experiments with immunodepletion, administration of pure, synthetic IAPP aggregates prepared in vitro, and aggregates of other disease-associated (Tau implicated in Alzheimer's disease) and nondisease–associated proteins (Mcc, a bacterial amyloid) clearly indicate that the active principle behind the pathologic transmission are the IAPP aggregates themselves. Our findings are in agreement with a recently published study by Oskarsson et al. (2015) in which Tg mice injected through the tail vein with in vitro–generated aggregates from synthetic peptides containing the sequence of IAPP developed a higher percentage of IAPP aggregates in the pancreas than did untreated controls when subjected to a high-fat diet.

Our ex vivo studies in islets were performed as a proof-of-concept demonstration to show that exogenously added aggregates of IAPP can induce formation of endogenous IAPP aggregates in an isolated system without any confounding physiologic variables. We used this paradigm following the field of neurodegenerative disorders associated to protein misfolding, in which a widely established method for studying propagation of protein aggregates in vitro consists of exposing cell lines to specific protein aggregates. Interestingly, isolated islets provide a superior platform for studying propagation of IAPP aggregates because islets retain the composition and organization of endocrine cells and the extracellular matrix, which is absent in isolated, cellular monolayers. Isolated islets also provide the unique possibility to work with human tissue, not genetically manipulated in any manner. The ex vivo model of IAPP-aggregate propagation developed in this work will provide an important platform to study the role of the extracellular matrix and cellular signaling mechanisms involved in the process of IAPP-aggregate propagation. The physiologic relevance of the findings obtained using ex vivo islet studies is demonstrated in the in vivo studies by administering IAPP aggregates, i.p., in living animals and monitoring the progressive accumulation of islet amyloid and associated diabetes pathology. We chose this route of administration in analogy to the prion field, in which most of the experiments to analyze prion infection by periphery are performed using this route of exposure. A similar experimental paradigm was recently used to test peripheral transmission potential of amyloid-β and Tau aggregates associated with Alzheimer's disease (Eisele et al., 2010; Clavaguera et al., 2014). In a future extension of our work, we plan to study in detail different routes of transmission, including oral administration and

staining (green). (B) The amyloid load present in the islets was quantified by measuring ThS-positive area/total islet area. The values correspond to means ± SE of 4–27 islets analyzed per condition. Data were analyzed by one-way ANOVA, and differences were highly significant ($P < 0.0001$). Individual differences among the different groups were studied by the Tukey's multiple comparison test. *, $P < 0.05$; ***, $P < 0.001$.

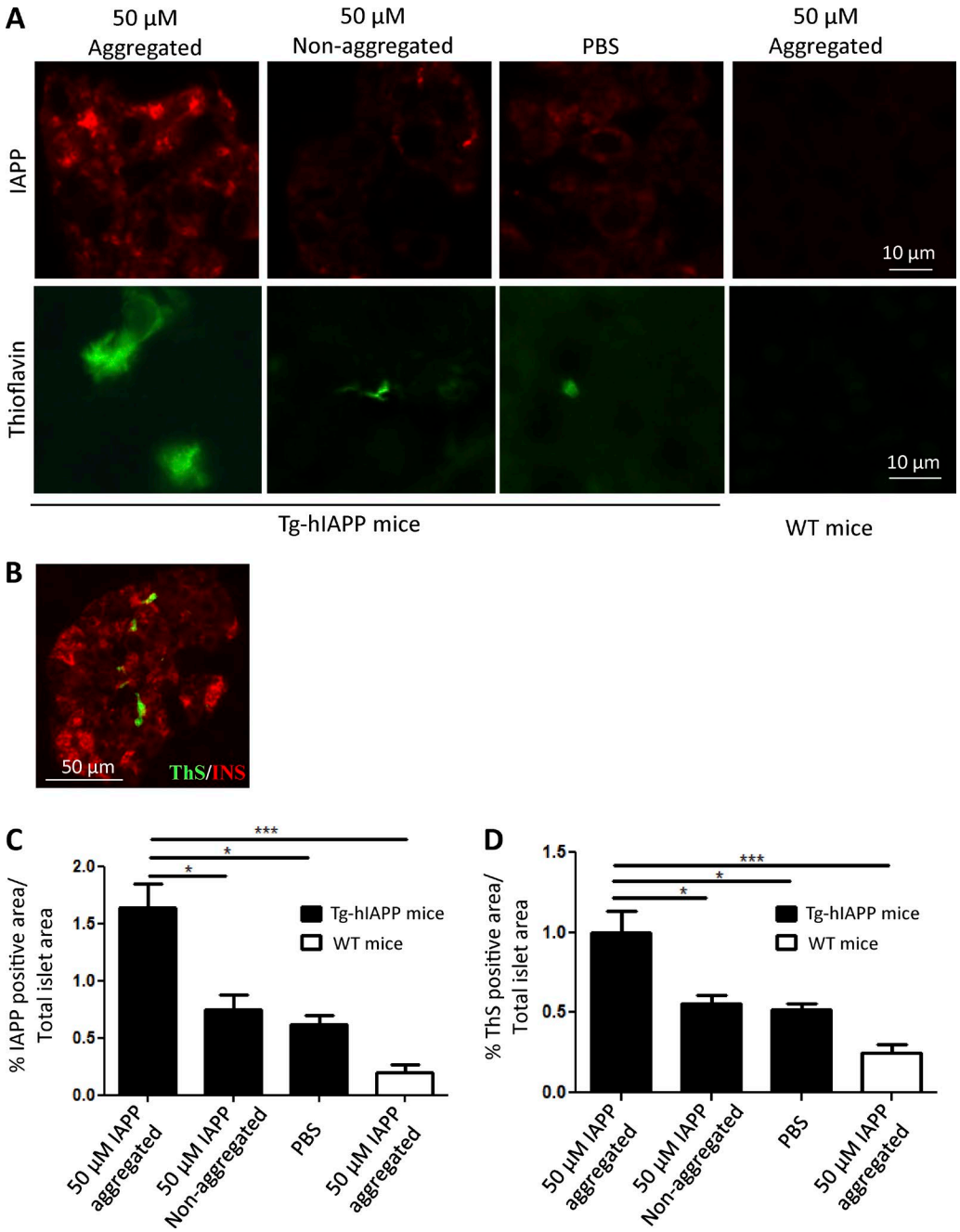

Figure 6. **In vivo induction of IAPP deposition by synthetic IAPP aggregates.** (See also Fig. S3.) (A) Groups of male, Tg-hIAPP mice were injected i.p. at 3 wk old with 50 µM of in vitro, prepared, synthetic IAPP aggregates or the same concentration of nonaggregated protein. Animals were sacrificed at 16 wk old, and appearance of IAPP aggregates was assessed by histologic studies using anti-IAPP antibody or the amyloid-binding dye ThS. The figures included correspond to representative pictures of the animals studied. As controls, WT mice were injected with the same preparation of synthetic IAPP aggregates. (B) Double-staining of ThS (green) and insulin (red). The picture corresponds to a representative image from one animal of the group treated with 50 µM of IAPP aggregates. The accumulation of aggregates was quantified by the area of the islets occupied by anti-IAPP antibody reactive (C) and ThS-positive (D) deposits. (C and D) Bars correspond to mean ± SE, and data were analyzed by one-way ANOVA, and in both cases, the differences were highly significant ($P < 0.001$). Individual differences among the groups were studied by the Tukey's multiple comparison posttest. *, $P < 0.05$; ***, $P < 0.001$.

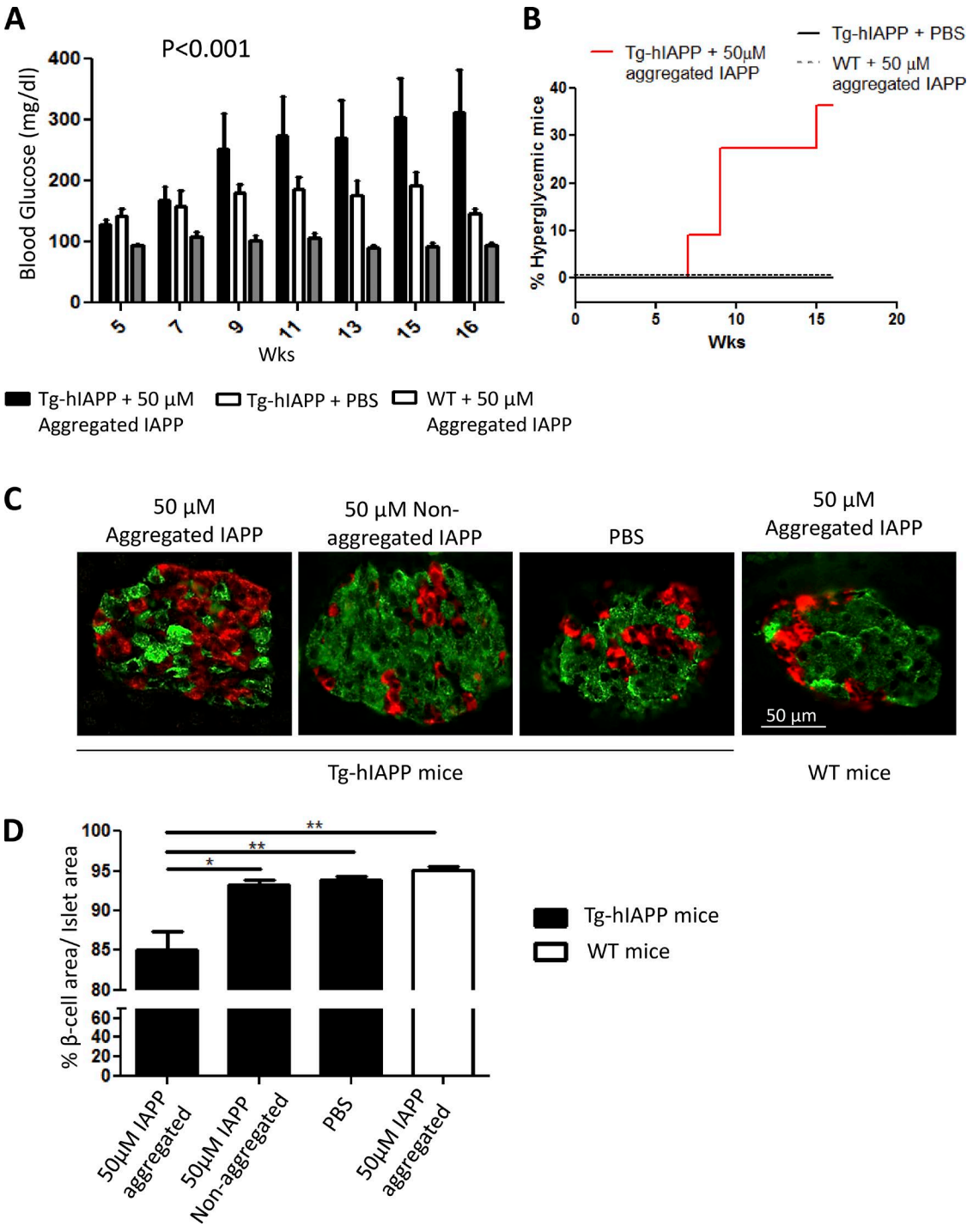

Figure 7. **Inoculation with synthetic IAPP aggregates induces clinical abnormalities typical of T2D.** (A) The fasting blood glucose concentration was measured over time in Tg-hIAPP or WT mice injected with synthetic IAPP aggregates or PBS. The values correspond to the means ± SE of the results obtained for 5–11 animals per group. Black bars represent the Tg-hIAPP mice inoculated with 50 µM of synthetic IAPP aggregates, and white bars are for the controls injected with PBS. Gray bars correspond to WT mice injected with the same preparation of IAPP aggregates. The data were statistically analyzed by two-way ANOVA using age and source of inoculation as the variables, and the results show a highly significant effect of the treatment ($P < 0.001$), but no significant effect on the interaction among the variables. (B) A proportion of Tg-hIAPP mice injected with IAPP aggregates developed severe hyperglycemia (>300 mg/dL), whereas none of the Tg mice treated with PBS were hyperglycemic. (C) The morphology and cellular composition of islets were measured in various groups of mice at 16 wk of age by staining with anti-insulin (green) or combined anti-glucagon and anti-somatostatin antibodies (red). Representative images of the islets from Tg-hIAPP mice treated with synthetic IAPP aggregates, the same quantity of nonaggregated protein, or the controls treated with

blood transfusion, two routes that have been shown to operate in prion diseases.

Another important conclusion of our studies from the point of understanding T2D is the potential role of IAPP misfolding and aggregation in the etiopathogenesis of the disease. Our results showing that induction of IAPP misfolding is sufficient to produce the main symptoms of the disease in the absence of any other process (such as high-fat diet or disruption of insulin signaling) suggest that IAPP misfolding and aggregation have an important role in the pathogenesis of T2D. This finding is consistent with previous observations indicating that in patients with diabetes, β cell pathology is observed selectively in islets containing IAPP aggregates (Jurgens et al., 2011). However, the extent to which spreading of IAPP aggregation may contribute to diabetic alterations needs to be further studied in more detail. In our studies, we observed hyperglycemia and impaired glucose tolerance in the Tg-hIAPP mice treated with IAPP aggregates, which occurred concomitant to a significant loss of β cells (>60%). Similar reduction of β cells has been associated with hyperglycemia in other rodent models as well as in patients affected by diabetes (Butler et al., 2003, 2004). Therefore, our results suggest that the hyperglycemia observed was due to the loss of β cells, which results in insufficient insulin secretion. Further experiments need to be performed to fully characterize the diabetic phenotype and the pathways implicated.

Finally, our data suggesting that some aspects of T2D pathology might be transmissible could open an entirely new area of research with profound implications for public health. Because IAPP aggregates are deposited in the periphery, the possibility that prion-like transmission events may occur is higher than in the neurodegenerative diseases, where the blood–brain barrier restricts exposure to peripherally acquired protein seeds to the brain. However, because until now this concept has not been considered, no epidemiologic studies have been performed to specifically analyze that possibility. Nevertheless, there are several articles suggesting an infectious-like pandemic increase in T2D incidence, although that is mostly attributed to changes in lifestyle and increases in obesity rates (Matthews and Matthews, 2011). In addition, several anecdotic studies have revealed an increased risk for diabetes after blood transfusion (Chern et al., 2001), organ transplant (Kasiske et al., 2003; Carey et al., 2012), or even maternal inheritance (Karter et al., 1999), which may suggest a possible transmission. However, considering the experimental nature of the models and conditions used in this study, the results should not be extrapolated to conclude that T2D is a transmissible disease in humans without additional studies. Perhaps of greater importance than a putative interindividual transmission, the prion phenomenon may have a key role in spreading the pathology from cell to cell or from islet to islet during the progression of the disease.

MATERIALS AND METHODS

IAPP Tg mice

As a model of IAPP aggregation, we used Tg mice overexpressing hIAPP at four- to fivefold levels of endogenous mouse IAPP (Janson et al., 1996). In homozygosis, male Tg mice spontaneously develop IAPP amyloid deposits, which are associated with selective β cell death, impaired insulin secretion and hyperglycemia (Janson et al., 1996). For all in vivo experiments, we used male mice because they all develop spontaneously pathological and clinical alterations of T2D, whereas females develop the abnormalities late and only a proportion of them develop the alterations. Animals were distributed randomly among the different groups. A colony of these animals was established in our facility after receiving breeding pairs from P.C. Butler (University of California, Los Angeles, Los Angeles, CA). Of note, the plasma glucose values obtained for our untreated Tg-hIAPP animals were a bit lower than those reported by Janson et al. (1996). This may be because our animals have undergone much subsequent breeding after the colony was provided by P.C. Butler. In Tg mice lines, it is not uncommon for the phenotype to gradually soften over time, most likely by a decrease in the number of copies of the transgene. Another possibility is that the food in our animal facility may have a different fat and/or carbohydrate composition than the one used by Janson and colleagues. All animal experiments were performed following US National Institutes of Health guidelines and were approved by the Animal Welfare Committee of the University of Texas Medical School, Houston.

Preparation of pancreas extracts

The pancreas of 12-mo-old, Tg-hIAPP mice, as well as age-matched WT mice of the same background, were extracted and immediately homogenized in 10% wt/vol PBS in the presence of a cocktail of protease inhibitors. Samples were sonicated to fully disaggregate the tissue. Material was kept frozen at −80°C until use.

Mouse islet isolation, homogenization, and culture

Islets from Tg-hIAPP, as well as controls, were isolated using a previously published procedure (Li et al., 2009). The pancreatic tissue was digested with collagenase IV for 15 min at 37°C. The digested material was recovered by centrifugation, washed in HBSS, and filtered through a 70-μm cell strainer. Finally, islets were separated from the remaining exocrine tissue by a Ficoll gradient, as previously described (Li et al., 2009). To prepare islet extracts, isolated islets were weighed

PBS. In addition, WT animals treated with the same preparation of synthetic IAPP aggregates are shown for comparison. Image analysis of stained islets was used to estimate the percentage of the islet area occupied by β cells (D) Data correspond to meand ± SE and were analyzed by one-way ANOVA, and differences were statistically significant (P = 0.0015). Individual differences were studied by the Tukey's multiple comparison test. *, P < 0.05; **, P < 0.01.

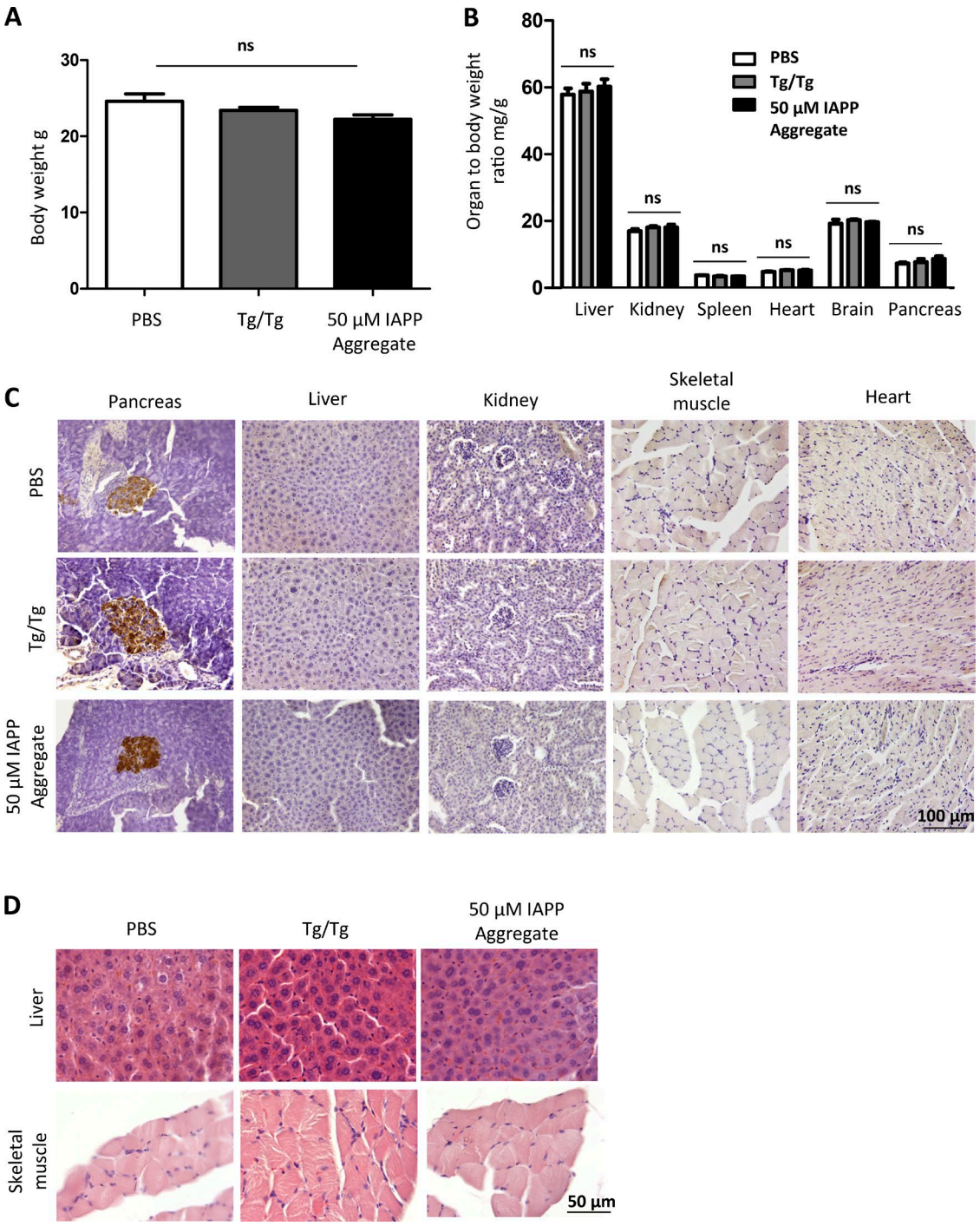

Figure 8. **Inoculation with IAPP aggregates does not induce toxicity and IAPP accumulation in major nonpancreatic tissues.** Groups of male, IAPP, Tg mice were injected i.p. at 4 wk of age with 10% pancreas homogenate from male, diabetic, IAPP Tg mice or 50 µM IAPP aggregates prepared from synthetic source. As a control, group of IAPP Tg mice were injected with PBS. (A) Body weight of injected animals was measured before sacrificing at 8 wk of age. Analysis by one-way ANOVA showed no significant ($P = 0.12$) changes in body weight because of injection of IAPP aggregates. (B) Represents the ratio of organ weight/body weight of animals injected with different inocula. The results shows that injection of IAPP aggregate-containing material, compared with PBS, does not induce significant changes in the weight of liver, kidney, spleen, heart, pancreas, and brain. Data for each organ was analyzed by one-way ANOVA, and no significant differences were observed in any of the tissues ($P > 0.05$). Bars in A and B correspond to mean ± SE. (C) Representative images of sections from different tissues stained with anti-IAPP antibody. The data show no IAPP accumulation in liver, kidney, skeletal muscle, and heart in any of the conditions tested. Sections from pancreas are shown as positive controls. (D) Representative images of sections from liver and skeletal muscle from different experimental groups, stained with hematoxylin and eosin, showing no gross morphological alterations.

and immediately frozen in liquid nitrogen and stored in −80°C. The stock was homogenized in PBS, using a mechanical Eppendorf homogenizer, to prepare 1% homogenate. For islet culture from Tg-hIAPP mice, isolated islets were cultured in RPMI-1640 (11875-083; Thermo Fisher Scientific), supplemented with 10% FBS, glutamine, and antibiotics at 37°C in 5% CO_2.

Human islet cultures

Human islets isolated postmortem from nondiabetic individuals were obtained from the National Disease Research Interchange. Protocols for sample collection were approved by the respective institutional review board of the National Disease Research Interchange. On arrival, islets were immediately placed in CMRL 1066 (Cellgro; Corning) enriched medium, supplemented with 2 mM L-glutamine (Cellgro CN- 25-005-CI; Corning), 1 mM sodium pyruvate, (Cellgro CN-25-000-CI; Corning), 10 mM Hepes-free acid, (Cellgro CN- 25-060-CI; Corning), 10 U/ml heparin (Hospira RL-4311; Pfizer), and 10 mM nicotinamide, (CN N0636; Sigma-Aldrich) at 24°C with 5% CO_2 for 7 d to stabilize the islets before starting the experiments. Studies were performed in the presence of 11 mM glucose in the medium.

Ex vivo experiments

Isolated islets were cultured in free-floating, 24-well ultralow attachment plates (07-200-602; Corning) with an approximate confluence of 50 islets/well. The total volume of medium per well was around 400 µl. Culture medium was changed every 5 d. After stabilization in the respective medium supplemented with 11 mM of glucose, islets were treated with 1% (or 0.1%) islet extracts from old Tg-hIAPP or WT controls with respect to the total volume of medium.

Immunodepletion experiments

Immunodepletion of IAPP from 1% islet homogenate of overtly diabetic Tg-hIAPP mice was performed in three successive rounds, using Dynabeads (Novex 11203D; Thermo Fisher Scientific) coupled with a cocktail of antibodies. For antibody coupling and immunodepletion, manufacturers' protocols were followed, except that 1 mg/ml BSA was used, instead of 0.1 mg/ml, for blocking unspecific interactions, and EDTA was removed from the beads during the final washing step. For the first round of depletion, beads coupled with N-terminal (1–13)–specific (T4153; Peninsula Laboratories International) and C-terminal (25–37)–specific (T4157; Peninsula Laboratories International) anti–hIAPP antibodies, 20 µg of each, were used. For the next two rounds, beads coupled with 1.5 µg of each N- and C-terminal–specific, anti–hIAPP antibodies and 1 µg of anti-oligomeric A11 antibody (AHB0052; Thermo Fisher Scientific) were used. After three rounds, the efficiency of depletion was tested by Western blot analysis using C-terminal (23–37)–specific anti–hIAPP antibody. Under those conditions, by measuring the pixel density of IAPP bands in Western blots (using ImageJ software; National Institutes of Health), we estimated that >70% of IAPP reactive bands were removed by the immunodepletion procedure.

Production of synthetic IAPP and preparation of aggregates

hIAPP containing the appropriate posttranslational modification (disulfide bridge and C-terminal amidation) was synthesized using solid-phase *N*-tert-butyloxycarbonyl chemistry at the W. Keck Facility at Yale University and was purified by reverse-phase HPLC. The final product was lyophilized and characterized by aa analysis and mass spectrometry. To prepare stock solutions free of IAPP-aggregated seeds, lyophilized, synthetic IAPP was dissolved in 2 mM HCl, and the resulting solution was sonicated and centrifuged at 16,000 *g* to remove existing aggregates. For ex vivo studies and i.p administration, the stock was diluted in PBS to the desired concentration. For in vitro seeding the stock was diluted in 100 mM Tris-HCl, pH 7.4 to reach the desired concentration. To produce IAPP aggregates, solutions of IAPP (0.2 mg/ml) in PBS were incubated overnight at 37°C with constant shaking at 500 revolutions per min (rpm). For the in vitro seeding assay, the stock solution of IAPP in 100 mM Tris-HCL was incubated at 25°C. The degree of aggregation was characterized by ThT fluorescence emission and electron microscopy after negative staining, as previously described (Salvadores et al., 2014).

Production of Tau and Mcc aggregates

Bacterial plasmid carrying the K18 fragment of human Tau containing four microtubule binding repeats (a gift from M. Margittai (University of Denver, Denver, CO) was overexpressed in Bl21 (D3) *Escherichia coli* bacteria and purified, as previously described (Meyer et al., 2014). K18 Tau aggregates were prepared by intermittent shaking (500 rpm) of 50 µM recombinant protein at 37°C in 100 mM Hepes, pH 7.4, containing 100 mM NaCl and 25 µM heparin. Mcc was purified from the culture supernatants of *E. coli* VCS257 cells harboring pJEM15 plasmid, as described earlier (Bieler et al., 2005). Mcc aggregates were prepared by constant shaking (500 rpm) of 100 µM purified protein at 37°C in 50 mM Pipes pH 6.5, containing 500 mM NaCl. The degree of aggregation was characterized by ThT fluorescence emission and electron microscopy after negative staining, as previously described (Bieler et al., 2005; Shahnawaz et al., 2017).

FTIR spectroscopy

FTIR experiments were conducted in an FT/IR-4100 spectrometer from Jasco Products. IAPP solution in PBS, after overnight aggregation, was centrifuged and resuspended to an estimated concentration of 5 mg/ml. 5 µl of aggregated protein slurry was then placed on the top of a diamond PRO450-S attenuated total reflectance unit from Jasco Products, adapted to the FT/IR-4100 system. Synthetic IAPP stock (5 mg/ml) was used as the soluble control. System parameters included 4.0 cm^{-1} resolution and an accumulation of 80 scans/sample. The data were processed using cosine

apodization and Mertz phase correction. The data were also corrected for attenuated total reflectance and carbon dioxide vapor absorption. Data fitting and secondary-structure calculations were analyzed, after corresponding buffer subtraction, by the secondary structure estimation 4000 software from Jasco Products. Each sample was measured in triplicate to confirm the secondary structure.

Induction of diabetes by STZ administration

To induce diabetes in WT mice, animals were treated with STZ, as previously described (Wilson and Leiter, 1990). In brief, STZ (Sigma-Aldrich) was diluted in sodium citrate buffer (10 mM, pH 4.5) and injected i.p. at 110 mg/kg per day for a consecutive 2 d. 1 mo after treatment, pancreas from fasted animals with a blood glucose level >500 mg/dL was collected and used as inoculum for i.p. injections.

Measurement of blood glycemia

Fasting blood glucose was monitored at various times after inoculation as indicated in the text. Mice were fasted for 16 h overnight, and blood sugar was measured using a Contour blood glucose monitoring system (Bayer). Blood was collected by venipuncture of the tail vein, and blood glucose was determined with a test strip inserted in the glucometer.

Glucose tolerance test

Mice were fasted for 16 h before the test. A glucose solution was injected i.p. (1 g/kg), and blood samples were taken by puncture of the tail vein at 0, 10, 20, 30, 60, 90, and 120 min after injection of glucose. Blood glucose levels were measured using a Contour blood glucose monitoring system (Bayer).

Histological analysis

Pancreas samples were fixed in 10% formaldehyde solution, embedded in paraffin, and sliced in 8-µm-thick sections. Four serial sections from each animal were stained with hematoxylin, ThS, or immunostained with various antibodies, including anti–hIAPP (27–37) polyclonal antibody (1:1000 dilution, Peninsula Laboratories International), anti-insulin antibody (1:1000; Abcam), anti-glucagon antibody (1:1000 dilution; Santa Cruz Biotechnology, Inc.) or anti-somatostatin antibody (1:1000 dilution; Santa Cruz Biotechnology, Inc.), using previously described protocols (Castilla et al., 2005; Moreno-Gonzalez et al., 2013). Immunoreactions were developed using a fluorescently labeled secondary antibody, and samples visualized in a Leica Biosystems epifluorescent microscope or using a secondary antibody linked to horseradish peroxidase and developed with a 3,3′-diaminobenzidine kit. The immunostained area was assessed in ≥25 islets from each animal. Images were submitted to image analysis using the image J software. To investigate the presence of IAPP accumulation and gross morphological abnormalities in nonpancreatic tissues, a section from the tissue was randomly chosen, and every tenth section was assessed (with a distance of 50 µm among them). Five sections per tissue were measured in each animal (n = 4–6/group).

Statistical analysis

The data were statistically analyzed by Student's t test, log-rank (Mantel–Cox) test, one-way or two-way ANOVA, followed by the Tukey's multiple comparison posttest, or the Kruskal–Wallis test, followed by Dunn's multiple comparison test. Statistical analysis was performed using the Prism software (version 5.0; GraphPad Software). The significance was set at 95% confidence.

Online supplemental material

Fig. S1 shows that WT mice inoculated with T2D Tg pancreas homogenate do not develop IAPP deposits or hyperglycemia. Fig. S2 shows that injection of pancreas homogenate from STZ-induced diabetic mice does not affect IAPP aggregation. Fig. S3 shows the preparation and characterization of synthetic IAPP aggregates in vitro. Fig. S4 shows the production and characterization of τ and Mcc fibrillar aggregates in vitro.

ACKNOWLEDGMENTS

We are very grateful to Dr. Peter C. Butler (University of California, Los Angeles, Los Angeles, CA) for supplying the colony of Tg-hIAPP mice used in this study and for providing advice in various aspects of IAPP and diabetes research. We thank Dr. Charles Mays and Marcelo Chacon in our laboratory for critical review and editing of the manuscript and Mrs. Andrea Flores for helping with maintaining and breeding animals for these experiments. We also thank Dr. Martin Margittai (University of Denver, Denver, CO) for providing the plasmid coding for Tau-4R.

The Integrated Microscopy Core was provided with funding from the Dan L. Duncan Cancer Center, Baylor College of Medicine, and the John S. Dunn Gulf Coast Consortium for Chemical Genomics for providing the electron microscopy micrographs. This study was supported in part by the Jeane B. Kempner postdoctoral fellowship awarded to A. Mukherjee.

The authors declare no competing financial interests.

Author contributions: A. Mukherjee participated in the characterization of the diabetic phenotype, completed the analysis of the in vivo study of IAPP administration of pancreatic aggregates, performed the characterization of IAPP toxicity and deposition in different organs, produced the final version of the figures, and prepared the draft of the manuscript. D. Morales-Scheihing performed most of the experiments with isolated islets and the in vivo experiments with synthetic IAPP aggregates. He also performed most of the histologic studies and participated in the preparation of the figures. N. Salvadores started the project and performed all initial in vivo experiments of transmission by administration of pancreatic homogenates and analyzed the results. I. Moreno-Gonzalez performed the in vivo experiment with STZ controls and collaborated with the histologic analysis. C. Gonzalez collaborated in the experiments with isolated islet cultures. K. Taylor-Presse collaborated with the experiments to analyze IAPP toxicity. N. Mendez purified and prepared aggregates of recombinant τ-4R and performed electron microscopy of IAPP aggregates. M. Shahnawaz purified and prepared aggregates of Mcc amyloid. A.O. Gaber, O.M. Sabek, and D.W. Fraga collaborated in the studies with human islet cultures. C. Soto is the principal investigator on the project and was responsible for coordinating research activity, analyzing the data, funding, writing the manuscript, and producing the final version of the article.

Submitted: 19 July 2016
Revised: 24 March 2017
Accepted: 19 June 2017

REFERENCES

Betsholtz, C., V. Svensson, F. Rorsman, U. Engström, G.T. Westermark, E. Wilander, K. Johnson, and P. Westermark. 1989. Islet amyloid polypeptide (IAPP): cDNA cloning and identification of an amyloidogenic region associated with the species-specific occurrence of age-related diabetes mellitus. *Exp. Cell Res.* 183:484–493. http://dx.doi.org/10.1016/0014-4827(89)90407-2

Bieler, S., L. Estrada, R. Lagos, M. Baeza, J. Castilla, and C. Soto. 2005. Amyloid formation modulates the biological activity of a bacterial protein. *J. Biol. Chem.* 280:26880–26885. http://dx.doi.org/10.1074/jbc.M502031200

Brissova, M., M.J. Fowler, W.E. Nicholson, A. Chu, B. Hirshberg, D.M. Harlan, and A.C. Powers. 2005. Assessment of human pancreatic islet architecture and composition by laser scanning confocal microscopy. *J. Histochem. Cytochem.* 53:1087–1097. http://dx.doi.org/10.1369/jhc.5C6684.2005

Brunham, L.R., J.K. Kruit, M.R. Hayden, and C.B. Verchere. 2010. Cholesterol in β-cell dysfunction: The emerging connection between HDL cholesterol and type 2 diabetes. *Curr. Diab. Rep.* 10:55–60. http://dx.doi.org/10.1007/s11892-009-0090-x

Butler, A.E., J. Janson, S. Bonner-Weir, R. Ritzel, R.A. Rizza, and P.C. Butler. 2003. β-Cell deficit and increased β-cell apoptosis in humans with type 2 diabetes. *Diabetes.* 52:102–110. http://dx.doi.org/10.2337/diabetes.52.1.102

Butler, A.E., J. Jang, T. Gurlo, M.D. Carty, W.C. Soeller, and P.C. Butler. 2004. Diabetes due to a progressive defect in β-cell mass in rats transgenic for human islet amyloid polypeptide (HIP rat): A new model for type 2 diabetes. *Diabetes.* 53:1509–1516. http://dx.doi.org/10.2337/diabetes.53.6.1509

Carey, E.J., B.A. Aqel, T.J. Byrne, D.D. Douglas, J. Rakela, H.E. Vargas, A.A. Moss, D.C. Mulligan, K.S. Reddy, and H.A. Chakkera. 2012. Pretransplant fasting glucose predicts new-onset diabetes after liver transplantation. *J. Transplant.* 2012:614781. http://dx.doi.org/10.1155/2012/614781

Castilla, J., P. Saá, C. Hetz, and C. Soto. 2005. In vitro generation of infectious scrapie prions. *Cell.* 121:195–206. http://dx.doi.org/10.1016/j.cell.2005.02.011

Chern, J.P., K.H. Lin, M.Y. Lu, D.T. Lin, K.S. Lin, J.D. Chen, and C.C. Fu. 2001. Abnormal glucose tolerance in transfusion-dependent β-thalassemic patients. *Diabetes Care.* 24:850–854. http://dx.doi.org/10.2337/diacare.24.5.850

Clark, A., C.A. Wells, I.D. Buley, J.K. Cruickshank, R.I. Vanhegan, D.R. Matthews, G.J. Cooper, R.R. Holman, and R.C. Turner. 1988. Islet amyloid, increased A-cells, reduced B-cells and exocrine fibrosis: quantitative changes in the pancreas in type 2 diabetes. *Diabetes Res.* 9:151–159.

Clavaguera, F., T. Bolmont, R.A. Crowther, D. Abramowski, S. Frank, A. Probst, G. Fraser, A.K. Stalder, M. Beibel, M. Staufenbiel, et al. 2009. Transmission and spreading of tauopathy in transgenic mouse brain. *Nat. Cell Biol.* 11:909–913. http://dx.doi.org/10.1038/ncb1901

Clavaguera, F., J. Hench, I. Lavenir, G. Schweighauser, S. Frank, M. Goedert, and M. Tolnay. 2014. Peripheral administration of τ aggregates triggers intracerebral tauopathy in transgenic mice. *Acta Neuropathol.* 127:299–301. http://dx.doi.org/10.1007/s00401-013-1231-5

de Koning, E.J., N.L. Bodkin, B.C. Hansen, and A. Clark. 1993. Diabetes mellitus in *Macaca mulatta* monkeys is characterised by islet amyloidosis and reduction in β-cell population. *Diabetologia.* 36:378–384. http://dx.doi.org/10.1007/BF00402271

Donath, M.Y., and S.E. Shoelson. 2011. Type 2 diabetes as an inflammatory disease. *Nat. Rev. Immunol.* 11:98–107. http://dx.doi.org/10.1038/nri2925

Eisele, Y.S., U. Obermüller, G. Heilbronner, F. Baumann, S.A. Kaeser, H. Wolburg, L.C. Walker, M. Staufenbiel, M. Heikenwalder, and M. Jucker. 2010. Peripherally applied Aβ-containing inoculates induce cerebral β-amyloidosis. *Science.* 330:980–982. http://dx.doi.org/10.1126/science.1194516

El-Assaad, W., J. Buteau, M.L. Peyot, C. Nolan, R. Roduit, S. Hardy, E. Joly, G. Dbaibo, L. Rosenberg, and M. Prentki. 2003. Saturated fatty acids synergize with elevated glucose to cause pancreatic β-cell death. *Endocrinology.* 144:4154–4163. http://dx.doi.org/10.1210/en.2003-0410

Fernández-Borges, N., H. Eraña, S.R. Elezgarai, C. Harrathi, M. Gayosso, and J. Castilla. 2013. Infectivity versus seeding in neurodegenerative diseases sharing a prion-like mechanism. *Int. J. Cell Biol.* 2013:583498. http://dx.doi.org/10.1155/2013/583498

Grad, L.I., W.C. Guest, A. Yanai, E. Pokrishevsky, M.A. O'Neill, E. Gibbs, V. Semenchenko, M. Yousefi, D.S. Wishart, S.S. Plotkin, and N.R. Cashman. 2011. Intermolecular transmission of superoxide dismutase 1 misfolding in living cells. *Proc. Natl. Acad. Sci. USA.* 108:16398–16403. http://dx.doi.org/10.1073/pnas.1102645108

Guest, W.C., J.M. Silverman, E. Pokrishevsky, M.A. O'Neill, L.I. Grad, and N.R. Cashman. 2011. Generalization of the prion hypothesis to other neurodegenerative diseases: an imperfect fit. *J. Toxicol. Environ. Health A.* 74:1433–1459. http://dx.doi.org/10.1080/15287394.2011.618967

Haataja, L., T. Gurlo, C.J. Huang, and P.C. Butler. 2008. Islet amyloid in type 2 diabetes, and the toxic oligomer hypothesis. *Endocr. Rev.* 29:303–316. http://dx.doi.org/10.1210/er.2007-0037

Höppener, J.W., B. Ahrén, and C.J. Lips. 2000. Islet amyloid and type 2 diabetes mellitus. *N. Engl. J. Med.* 343:411–419. http://dx.doi.org/10.1056/NEJM200008103430607

Howard, C.F. Jr. 1986. Longitudinal studies on the development of diabetes in individual *Macaca nigra*. *Diabetologia.* 29:301–306. http://dx.doi.org/10.1007/BF00452067

Hull, R.L., G.T. Westermark, P. Westermark, and S.E. Kahn. 2004. Islet amyloid: a critical entity in the pathogenesis of type 2 diabetes. *J. Clin. Endocrinol. Metab.* 89:3629–3643. http://dx.doi.org/10.1210/jc.2004-0405

Iba, M., J.L. Guo, J.D. McBride, B. Zhang, J.Q. Trojanowski, and V.M. Lee. 2013. Synthetic τ fibrils mediate transmission of neurofibrillary tangles in a transgenic mouse model of Alzheimer's-like tauopathy. *J. Neurosci.* 33:1024–1037. http://dx.doi.org/10.1523/JNEUROSCI.2642-12.2013

Janson, J., W.C. Soeller, P.C. Roche, R.T. Nelson, A.J. Torchia, D.K. Kreutter, and P.C. Butler. 1996. Spontaneous diabetes mellitus in transgenic mice expressing human islet amyloid polypeptide. *Proc. Natl. Acad. Sci. USA.* 93:7283–7288. http://dx.doi.org/10.1073/pnas.93.14.7283

Janson, J., R.H. Ashley, D. Harrison, S. McIntyre, and P.C. Butler. 1999. The mechanism of islet amyloid polypeptide toxicity is membrane disruption by intermediate-sized toxic amyloid particles. *Diabetes.* 48:491–498. http://dx.doi.org/10.2337/diabetes.48.3.491

Johnson, K.H., T.D. O'Brien, C. Betsholtz, and P. Westermark. 1989. Islet amyloid, islet-amyloid polypeptide, and diabetes mellitus. *N. Engl. J. Med.* 321:513–518. http://dx.doi.org/10.1056/NEJM198908243210806

Jucker, M., and L.C. Walker. 2013. Self-propagation of pathogenic protein aggregates in neurodegenerative diseases. *Nature.* 501:45–51. http://dx.doi.org/10.1038/nature12481

Jurgens, C.A., M.N. Toukatly, C.L. Fligner, J. Udayasankar, S.L. Subramanian, S. Zraika, K. Aston-Mourney, D.B. Carr, P. Westermark, G.T. Westermark, et al. 2011. β-cell loss and β-cell apoptosis in human type 2 diabetes are related to islet amyloid deposition. *Am. J. Pathol.* 178:2632–2640. http://dx.doi.org/10.1016/j.ajpath.2011.02.036

Kahn, S.E. 2003. The relative contributions of insulin resistance and β-cell dysfunction to the pathophysiology of Type 2 diabetes. *Diabetologia.* 46:3–19. http://dx.doi.org/10.1007/s00125-002-1009-0

Karter, A.J., S.E. Rowell, L.M. Ackerson, B.D. Mitchell, A. Ferrara, J.V. Selby, and B. Newman. 1999. Excess maternal transmission of type 2 diabetes: The Northern California Kaiser Permanente Diabetes Registry. *Diabetes Care.* 22:938–943. http://dx.doi.org/10.2337/diacare.22.6.938

Kasiske, B.L., J.J. Snyder, D. Gilbertson, and A.J. Matas. 2003. Diabetes mellitus after kidney transplantation in the United States. *Am. J. Transplant.* 3:178–185. http://dx.doi.org/10.1034/j.1600-6143.2003.00010.x

Kharouta, M., K. Miller, A. Kim, P. Wojcik, G. Kilimnik, A. Dey, D.F. Steiner, and M. Hara. 2009. No mantle formation in rodent islets -- The prototype of islet revisited. *Diabetes Res. Clin. Pract.* 85:252–257. http://dx.doi.org/10.1016/j.diabres.2009.06.021

Levine, H. III. 1993. Thioflavine T interaction with synthetic Alzheimer's disease β-amyloid peptides: Detection of amyloid aggregation in solution. *Protein Sci.* 2:404–410. http://dx.doi.org/10.1002/pro.5560020312

Li, D.S., Y.H. Yuan, H.J. Tu, Q.L. Liang, and L.J. Dai. 2009. A protocol for islet isolation from mouse pancreas. *Nat. Protoc.* 4:1649–1652. http://dx.doi.org/10.1038/nprot.2009.150

Luheshi, L.M., D.C. Crowther, and C.M. Dobson. 2008. Protein misfolding and disease: from the test tube to the organism. *Curr. Opin. Chem. Biol.* 12:25–31. http://dx.doi.org/10.1016/j.cbpa.2008.02.011

Luk, K.C., V. Kehm, J. Carroll, B. Zhang, P. O'Brien, J.Q. Trojanowski, and V.M. Lee. 2012. Pathological α-synuclein transmission initiates Parkinson-like neurodegeneration in nontransgenic mice. *Science.* 338:949–953. http://dx.doi.org/10.1126/science.1227157

Lundmark, K., G.T. Westermark, S. Nyström, C.L. Murphy, A. Solomon, and P. Westermark. 2002. Transmissibility of systemic amyloidosis by a prion-like mechanism. *Proc. Natl. Acad. Sci. USA.* 99:6979–6984. (published erratum appears in *Proc. Natl. Acad. Sci. USA.* 2003. http://dx.doi.org/10.1073/pnas.0630139100) http://dx.doi.org/10.1073/pnas.092205999

Ma, Z., G.T. Westermark, K.H. Johnson, T.D. O'Brien, and P. Westermark. 1998. Quantitative immunohistochemical analysis of islet amyloid polypeptide (IAPP) in normal, impaired glucose tolerant, and diabetic cats. *Amyloid.* 5:255–261. http://dx.doi.org/10.3109/13506129809007298

Matthews, D.R., and P.C. Matthews. 2011. Banting Memorial Lecture 2010^. Type 2 diabetes as an 'infectious' disease: Is this the Black Death of the 21st century? *Diabet. Med.* 28:2–9. http://dx.doi.org/10.1111/j.1464-5491.2010.03167.x

Meyer, V., P.D. Dinkel, E. Rickman Hager, and M. Margittai. 2014. Amplification of T fibrils from minute quantities of seeds. *Biochemistry.* 53:5804–5809. http://dx.doi.org/10.1021/bi501050g

Meyer-Luehmann, M., J. Coomaraswamy, T. Bolmont, S. Kaeser, C. Schaefer, E. Kilger, A. Neuenschwander, D. Abramowski, P. Frey, A.L. Jaton, et al. 2006. Exogenous induction of cerebral β-amyloidogenesis is governed by agent and host. *Science.* 313:1781–1784. http://dx.doi.org/10.1126/science.1131864

Morales, R., C. Duran-Aniotz, J. Castilla, L.D. Estrada, and C. Soto. 2012. De novo induction of amyloid-β deposition in vivo. *Mol. Psychiatry.* 17:1347–1353. http://dx.doi.org/10.1038/mp.2011.120

Moreno-Gonzalez, I., L.D. Estrada, E. Sanchez-Mejias, and C. Soto. 2013. Smoking exacerbates amyloid pathology in a mouse model of Alzheimer's disease. *Nat. Commun.* 4:1495. http://dx.doi.org/10.1038/ncomms2494

Mougenot, A.L., S. Nicot, A. Bencsik, E. Morignat, J. Verchère, L. Lakhdar, S. Legastelois, and T. Baron. 2012. Prion-like acceleration of a synucleinopathy in a transgenic mouse model. *Neurobiol. Aging.* 33:2225–2228. http://dx.doi.org/10.1016/j.neurobiolaging.2011.06.022

Mukherjee, A., D. Morales-Scheihing, P.C. Butler, and C. Soto. 2015. Type 2 diabetes as a protein misfolding disease. *Trends Mol. Med.* 21:439–449. http://dx.doi.org/10.1016/j.molmed.2015.04.005

Novials, A., I. Rojas, R. Casamitjana, E.F. Usac, and R. Gomis. 2001. A novel mutation in islet amyloid polypeptide (IAPP) gene promoter is associated with type II diabetes mellitus. *Diabetologia.* 44:1064–1065.

Nyalakonda, K., T. Sharma, and F. Ismail-Beigi. 2010. Preservation of β-cell function in type 2 diabetes. *Endocr. Pract.* 16:1038–1055. http://dx.doi.org/10.4158/EP10112.RA

Oskarsson, M.E., J.F. Paulsson, S.W. Schultz, M. Ingelsson, P. Westermark, and G.T. Westermark. 2015. In vivo seeding and cross-seeding of localized amyloidosis: A molecular link between type 2 diabetes and Alzheimer disease. *Am. J. Pathol.* 185:834–846. http://dx.doi.org/10.1016/j.ajpath.2014.11.016

Paulsson, J.F., J. Ludvigsson, A. Carlsson, R. Casas, G. Forsander, S.A. Ivarsson, I. Kockum, Å. Lernmark, C. Marcus, B. Lindblad, and G.T. Westermark. 2014. High plasma levels of islet amyloid polypeptide in young with new-onset of type 1 diabetes mellitus. *PLoS One.* 9:e93053. http://dx.doi.org/10.1371/journal.pone.0093053

Piccardo, P., D. King, G. Telling, J.C. Manson, and R.M. Barron. 2013. Dissociation of prion protein amyloid seeding from transmission of a spongiform encephalopathy. *J. Virol.* 87:12349–12356. http://dx.doi.org/10.1128/JVI.00673-13

Poitout, V., and R.P. Robertson. 2002. Minireview: secondary β-cell failure in type 2 diabetes--A convergence of glucotoxicity and lipotoxicity. *Endocrinology.* 143:339–342. http://dx.doi.org/10.1210/endo.143.2.8623

Polonsky, K.S. 2000. Dynamics of insulin secretion in obesity and diabetes. *Int. J. Obes. Relat. Metab. Disord.* 24:S29–S31. http://dx.doi.org/10.1038/sj.ijo.0801273

Prusiner, S.B. 1998. Prions. *Proc. Natl. Acad. Sci. USA.* 95:13363–13383. http://dx.doi.org/10.1073/pnas.95.23.13363

Prusiner, S.B. 2012. Cell biology: A unifying role for prions in neurodegenerative diseases. *Science.* 336:1511–1513. http://dx.doi.org/10.1126/science.1222951

Ren, P.H., J.E. Lauckner, I. Kachirskaia, J.E. Heuser, R. Melki, and R.R. Kopito. 2009. Cytoplasmic penetration and persistent infection of mammalian cells by polyglutamine aggregates. *Nat. Cell Biol.* 11:219–225. http://dx.doi.org/10.1038/ncb1830

Ritzel, R.A., and P.C. Butler. 2003. Replication increases β-cell vulnerability to human islet amyloid polypeptide-induced apoptosis. *Diabetes.* 52:1701–1708. http://dx.doi.org/10.2337/diabetes.52.7.1701

Salvadores, N., M. Shahnawaz, E. Scarpini, F. Tagliavini, and C. Soto. 2014. Detection of misfolded Aβ oligomers for sensitive biochemical diagnosis of Alzheimer's disease. *Cell Reports.* 7:261–268. http://dx.doi.org/10.1016/j.celrep.2014.02.031

Schmidt, C., A. Karch, C. Korth, and I. Zerr. 2012. On the issue of transmissibility of Alzheimer disease: A critical review. *Prion.* 6:447–452. http://dx.doi.org/10.4161/pri.22502

Shahnawaz, M., K.W. Park, A. Mukherjee, R. Diaz-Espinoza, and C. Soto. 2017. Prion-like characteristics of the bacterial protein Microcin E492. *Sci. Rep.* 7:45720. http://dx.doi.org/10.1038/srep45720

Shammas, S.L., G.A. Garcia, S. Kumar, M. Kjaergaard, M.H. Horrocks, N. Shivji, E. Mandelkow, T.P. Knowles, E. Mandelkow, and D. Klenerman. 2015. A mechanistic model of τ amyloid aggregation based on direct observation of oligomers. *Nat. Commun.* 6:7025. http://dx.doi.org/10.1038/ncomms8025

Siddiqua, A., and M. Margittai. 2010. Three- and four-repeat T coassemble into heterogeneous filaments: An implication for Alzheimer disease. *J. Biol. Chem.* 285:37920–37926. http://dx.doi.org/10.1074/jbc.M110.185728

Soto, C. 2003. Unfolding the role of protein misfolding in neurodegenerative diseases. *Nat. Rev. Neurosci.* 4:49–60. http://dx.doi.org/10.1038/nrn1007

Soto, C. 2012. Transmissible proteins: expanding the prion heresy. *Cell.* 149:968–977. http://dx.doi.org/10.1016/j.cell.2012.05.007

Soto, C., and L.D. Estrada. 2008. Protein misfolding and neurodegeneration. *Arch. Neurol.* 65:184–189. http://dx.doi.org/10.1001/archneurol.2007.56

Soto, C., L. Estrada, and J. Castilla. 2006. Amyloids, prions and the inherent infectious nature of misfolded protein aggregates. *Trends Biochem. Sci.* 31:150–155. http://dx.doi.org/10.1016/j.tibs.2006.01.002

Stöhr, J., J.C. Watts, Z.L. Mensinger, A. Oehler, S.K. Grillo, S.J. DeArmond, S.B. Prusiner, and K. Giles. 2012. Purified and synthetic Alzheimer's amyloid β (Aβ) prions. *Proc. Natl. Acad. Sci. USA.* 109:11025–11030. http://dx.doi.org/10.1073/pnas.1206555109

Stumvoll, M., B.J. Goldstein, and T.W. van Haeften. 2005. Type 2 diabetes: Principles of pathogenesis and therapy. *Lancet.* 365:1333–1346. http://dx.doi.org/10.1016/S0140-6736(05)61032-X

Walsh, D.M., and D.J. Selkoe. 2016. A critical appraisal of the pathogenic protein spread hypothesis of neurodegeneration. *Nat. Rev. Neurosci.* 17:251–260. http://dx.doi.org/10.1038/nrn.2016.13

Westermark, P. 1972. Quantitative studies on amyloid in the islets of Langerhans. *Ups. J. Med. Sci.* 77:91–94. http://dx.doi.org/10.1517/03009734000000014

Westermark, P., U. Engström, K.H. Johnson, G.T. Westermark, and C. Betsholtz. 1990. Islet amyloid polypeptide: Pinpointing amino acid residues linked to amyloid fibril formation. *Proc. Natl. Acad. Sci. USA.* 87:5036–5040. http://dx.doi.org/10.1073/pnas.87.13.5036

Wilson, G.L., and E.H. Leiter. 1990. Streptozotocin interactions with pancreatic β cells and the induction of insulin-dependent diabetes. *Curr. Top. Microbiol. Immunol.* 156:27–54.

Xing, Y., A. Nakamura, T. Chiba, K. Kogishi, T. Matsushita, F. Li, Z. Guo, M. Hosokawa, M. Mori, and K. Higuchi. 2001. Transmission of mouse senile amyloidosis. *Lab. Invest.* 81:493–499. http://dx.doi.org/10.1038/labinvest.3780257

Yang, H., S. Yang, J. Kong, A. Dong, and S. Yu. 2015. Obtaining information about protein secondary structures in aqueous solution using Fourier transform IR spectroscopy. *Nat. Protoc.* 10:382–396. http://dx.doi.org/10.1038/nprot.2015.024

Zraika, S., R.L. Hull, J. Udayasankar, K.M. Utzschneider, J. Tong, F. Gerchman, and S.E. Kahn. 2007. Glucose- and time-dependence of islet amyloid formation in vitro. *Biochem. Biophys. Res. Commun.* 354:234–239. http://dx.doi.org/10.1016/j.bbrc.2006.12.187